Pre-Cadomian to late-Variscan odyssey of the eastern Massif Central, France: Formation of the West European crust in a nutshell

Cyril Chelle-Michou, Oscar Laurent, Jean-François Moyen, Sylvain Block, Jean-Louis Paquette, Simon Couzinié, Véronique Gardien, Olivier Vanderhaeghe, Arnaud Villaros, Armin Zeh

Pre-Cadomian to late-Variscan odyssey of the eastern Massif Central, France: Formation of the West European crust in a nutshell

Cyril Chelle-Michou, Oscar Laurent, Jean-François Moyen, Sylvain Block, Jean-Louis Paquette, Simon Couzinié, Véronique Gardien, Olivier Vanderhaeghe, Arnaud Villaros, Armin Zeh

PII: S1342-937X(16)30159-9
DOI: doi: 10.1016/j.gr.2017.02.010
Reference: GR 1752

To appear in:

Received date: 24 August 2016
Revised date: 1 February 2017
Accepted date: 14 February 2017

Please cite this article as: Cyril Chelle-Michou, Oscar Laurent, Jean-François Moyen, Sylvain Block, Jean-Louis Paquette, Simon Couzinié, Véronique Gardien, Olivier Vanderhaeghe, Arnaud Villaros, Armin Zeh , Pre-Cadomian to late-Variscan odyssey of the eastern Massif Central, France: Formation of the West European crust in a nutshell. The address for the corresponding author was captured as affiliation for all authors. Please check if appropriate. Gr(2017), doi: 10.1016/j.gr.2017.02.010

Pre-Cadomian to late-Variscan odyssey of the eastern Massif Central, France: formation of the West European crust in a nutshell

Cyril Chelle-Michou[1,2*], Oscar Laurent[3,4], Jean-François Moyen[2], Sylvain Block[5], Jean-Louis Paquette[6], Simon Couzinié[2], Véronique Gardien[7], Olivier Vanderhaeghe[5], Arnaud Villaros[8], Armin Zeh[3,9]

[1] *Department of Earth Sciences, University of Geneva, rue des Maraîchers 13, CH-1205 Geneva, Switzerland*

[2] *Univ. Lyon, UJM-Saint-Etienne, UBP, CNRS, IRD, Laboratoire Magmas et Volcans UMR 6524, F-42023 Saint Etienne, France*

[3] *Institut für Geowissenschaften, J.W. Goethe Universität, Altenho□ferallee 1, D-60438 Frankfurt, Germany*

[4] *Université de Liège, Département de Géologie B20, Quartier Agora, Allée du six-Août 12, B-4000 Liège, Belgium*

[5] *Géosciences Environnement Toulouse (GET), Université de Toulouse, CNRS, IRD, 14, Avenue Edouard Belin, F-31400 Toulouse, France*

[6] *Laboratoire Magmas et Volcans, Université Clermont-Auvergne, CNRS-IRD-OPGC, F-63000 Clermont-Ferrand, France*

[7] *Laboratoire de Géologie de Lyon (CNRS UMR 5276), Université Lyon 1/ENS Lyon, Campus de la Doua, 2 rue Raphae□l Dubois, F-69622 Villeurbanne Cedex, France*

[8] *Institut des Sciences de la Terre d'Orléans (ISTO), Université d'Orléans, CNRS UMR 7327, 1A rue de la Férollerie, F-45071 Orléans cedex 2, France*

[9] *Institut für Angewandte Geowissenschaften, Karlsruher Institut für Technologie, Mineralogie und Petrologie, Adenauerring 20b, D-76131 Karlsruhe, Germany*

* Corresponding author: cyril.chelle-michou@bristol.ac.uk

School of Earth Sciences, University of Bristol, Wills Memorial Building, Queens Road, Bristol BS8 1RJ, UK

Abstract

The East Massif Central (EMC), France, is part of the internal zone of the Variscan belt where late Carboniferous crustal melting and orogenic collapse have largely obliterated the pre- to early-Variscan geological record. Nevertheless, parts of this history can be reconstructed by using *in-situ* U-Th-Pb-Lu-Hf isotopic data of texturally well-defined zircon grains from different lithological units. All the main rock units commonly described in the EMC are present in the area of Tournon and include meta-sedimentary and meta-igneous rocks of the Upper Gneiss Unit (UGU) and of the Lower Gneiss Unit (LGU), as well as cross-cutting Variscan granitoid dikes and a heterogeneous granite coring the major Velay dome. Herein we demonstrate that the UGU and the LGU have markedly distinct zircon records. The results of this study are consistent with deposition of the protoliths of the paragneisses within a back-arc basin that was located adjacent to the Arabian-Nubian shield and/or the Saharan Metacraton during the late Ediacaran and collected detritus from the Gondwana continent. At ~545 Ma some of these sedimentary rocks were affected by a first melting event that formed the protoliths of the LGU orthogneisses, those of which subsequently remelted at ca. 308 Ma to form the Velay granite-migmatite dome. Protoliths of the UGU result mainly from a bimodal rift-related magmatism at ~480 Ma, corresponding to melting of the Ediacaran sediments and depleted mantle. Zircon rims from the UGU additionally provide evidence for a metamorphic/migmatitic overprint during the Lower Carboniferous (~350–340 Ma). Finally, several generations of granite dikes of which inherited zircons display characteristics of both the UGU and the LGU were protractedly emplaced from ~322 Ma to ~308 Ma, the youngest of which being coeval with the formation of the Velay dome. Our data further show that the vast majority of crustal material ultimately involved in the Variscan orogeny, which forms the present-day basement in the EMC, was derived from a sedimentary mixture of

various components from the Gondwana continent deposited in Ediacaran times, with no evidence for the involvement of an older autochthonous crust.

Keywords: North Gondwana margin; Variscan orogeny; Massif Central; Pan-African/Cadomian orogenies; Zircon

1. Introduction

The Variscan orogen provides record of Lower Devonian to the Upper Carboniferous collisions between Gondwana, Laurussia and several intervening Gondwana-derived microcontinental terranes (Matte, 2001; Simancas et al., 2005; von Raumer et al., 2003). These collisions resulted in the amalgamation of the supercontinent Pangea, and in the formation of a vast mountain belt, the amplitude of which is often compared to that of the modern-day Himalayas (Dewey and Burke, 1973; Kroner and Romer, 2013; Ménard and Molnar, 1988; Stampfli et al., 2013) although such a comparison has recently be questioned (Franke, 2014). The French Massif Central is one of the largest Variscan massifs and represents the exhumed internal zone of the orogen (e.g., Lardeaux et al., 2014; Fig. 1), thus offering insightful opportunities to study geologic processes that were at play in the Variscan orogenic core. In addition, pre-Variscan relicts (mostly gneisses and schists) of the eastern Massif Central (EMC; Fig. 1) are intimately associated with the Variscan granitoids and can further provide insight into the evolution of pre-Variscan terranes (i.e., timing of crustal formation and reworking, related geodynamic settings, and paleo-geographic positions) and into their role into the Variscan orogeny. Ultimately, the study of the EMC can provide a time transgressive window to study the protracted evolution of the local crust.

Zircon has proven to be a resistant mineral in a range of extreme geological processes from the surface to the deep Earth crust (e.g., Harley and Kelly, 2007). U-Pb dating of zircon

is considered to be one of the most robust techniques for dating magmatic and metamorphic events (e.g., Corfu, 2013). In addition, combined U-Pb dating and Hf isotope analyses of zircon can provide key information regarding the source of the magma from which zircon crystallized as well as on the timing of crustal formation and reworking (Condie et al., 2011; Kemp et al., 2006). Moreover, combined U–Pb dating and Hf isotope tracing has proven efficient in retrieving reliable chrono-petrological information even from complexly zoned zircons grains formed and/or altered during multiple metamorphic, magmatic, and/or sedimentary processes (e.g., Gerdes and Zeh, 2009; Kemp et al., 2006; 2009; Zeh et al., 2010a, 2010b). As a result, zircon is the perfect tool to investigate crustal evolution in the eastern Massif Central (EMC; Fig. 1) where very intense late-Variscan partial-melting and magmatism has significantly disrupted most of the pre-Variscan rock record.

Compared with other Variscan massifs such as Bohemia and Iberia, the EMC has been the subject of relatively few modern geochronological studies. The specific timing of pre- and syn-Variscan tectono-magmatic events, and their associated geodynamic–paleogeographic environments therefore remain poorly defined within the area. Herein, we present an integrated U–Pb dating (n = 771) and Hf isotopic (n = 339) study of magmatic, detrital and metamorphic zircon grains/domains from the Tournon area of the EMC (Figs. 1, 2). The Tournon area presents a complete cross-section through the classically described nappe pile and crosscutting magmatic rocks of the EMC (Lardeaux et al., 2014; Ledru et al., 1989). The area therefore represents a key locality for study of both the pre- and syn-Variscan history of the EMC. Our sampling strategy was designed to encompass the main lithological units within the Tournon area that are representative across the EMC. The new data are used to constrain the Precambrian paleogeographic position of the Massif Central terrane, to discuss the evolution of the north Gondwana margin throughout the Cadomian and Variscan orogenies and to provide a synoptic timeframe for Variscan magmatic and metamorphic

events in the EMC. Finally, we discuss the genesis and reworking of the western European continental crust.

2. Geological background

The EMC is characterized by a south-verging Devonian to early Carboniferous stack of metamorphic nappes (Faure et al., 2009; Lardeaux et al., 2014; Ledru et al., 1989) that was dismantled by late Carboniferous strike-slip tectonics and magmatism associated with late-orogenic extension and collapse (Faure, 1995; Vanderhaeghe et al., 1999). The highest structural level within the nappe stack is represented by the Brévenne unit (Fig. 1), which consists of greenschist facies Upper Devonian (ca. 365 Ma) calc-alkaline to tholeiitic volcanic and volcano-clastic rocks emplaced in an immature back-arc setting (Feybesse et al., 1988; Lardeaux et al., 2014; Pin and Paquette, 1997; Sider and Ohnenstetter, 1986).

South of (and structurally below) the Brévenne Unit, the "Upper Gneiss Unit" (UGU; Fig. 1) is characterized by ortho- and paragneisses (with Cambrian to Ordovician protoliths) containing high-pressure (HP) and high-temperature (HT) relicts (eclogite and granulite) (Gardien, 1993; Gardien et al., 1990; Lardeaux et al., 2001; Ledru et al., 1989). A Lower Ordovician bimodal magmatic association, the so-called "Leptyno-Amphibolitic Complex" (LAC), forms the characteristic base of the UGU (Briand et al., 1991; Pin and Lancelot, 1982; Santallier et al., 1988). The LAC is interpreted to represent remnants of thinned continental lithosphere with local oceanic affinities (ultra-basic rocks and tholeiitic metabasalts/metagabbros) (Briand et al., 1991; Gardien et al., 1990; Lardeaux et al., 2014; Pin, 1990; Pin and Paquette, 1997), the so-called Galicia-Massif Central oceanic domain(s). Dates between 432 and 408 Ma (ID-TIMS U-Pb on multigrain zircon fractions, LA-ICPMS U-Pb on zircon, and EMPA U-Th-Pb on monazite) on eclogite and granulite samples have been attributed to HP metamorphism (Berger et al., 2010; Do Couto et al., 2015; Ducrot et al.,

1983; Paquette et al., 1995; Pin and Lancelot, 1982) related to early Variscan subduction of this(ese) oceanic domain(s) (Faure et al., 2009; Ledru et al., 1989; Matte, 1991). Subsequently, exhumation of the UGU in the northern part of the Massif Central was driven by isothermal decompression accompanied by anatexis between 389 and 375 Ma (Boutin and Montigny, 1993; Costa and Maluski, 1988; Duthou et al., 1994). Available data suggest that exhumation of the UGU was diachronous from north to south: while in the northern part (Lyonnais area, Northeast of St-Etienne, Fig. 1), the UGU had cooled below 300°C by 350-340 Ma ($^{40}Ar/^{39}Ar$ data on amphibole, biotite and muscovite; Costa et al., 1993), partial melting of the UGU during exhumation was ongoing at 345 ± 10 Ma in the southern Massif Central (Pin and Lancelot, 1982). This event likely corresponds to the stacking of the UGU nappe(s) atop the Lower Gneiss Unit (see below).

The "Lower Gneiss Unit" (LGU), largely crops out South of the Pilat low-angle detachment (controlling the development of the late Carboniferous St-Etienne coal basin; Fig. 1). It consists of orthogneisses (peraluminous metagranite and metarhyolite), paragneisses, and minor amphibolites with dominantly Cambrian protoliths (Caen-Vachette, 1979; Mintrone, 2015; R'Kha Chaham et al., 1990). Following amphibolite facies metamorphism, rocks of the LGU were affected by a major late Carboniferous HT-LP event, marked by widespread crustal melting that led to the formation of the Velay granite-migmatite dome (Barbey et al., 1999; 2015; Burg and Vanderhaeghe, 1993; Couzinié et al., 2014; Dupraz and Didier, 1988; Gardien et al., 1997; Ledru et al., 2001; Montel et al., 1992; Vanderhaeghe et al., 1999). In contrast to the UGU, the LGU does not record a HP event in the EMC.

The area south of the Velay granite-migmatite dome consists of greenschist to lower-amphibolite facies metasediments belonging to the "Para-autochtonous Unit" (Fig. 1). Metamorphism was polyphased from ca. 340 to 310 Ma and related to thrusting, granite emplacement and the far field effect of the Velay granite-migmatite dome (Bouilhol et al.,

2006; Faure et al., 2001). It has been suggested that these metasediments were deposited along the North Gondwana margin, presumably from the Ediacaran through the Lower Cambrian (Melleton et al., 2010).

Voluminous granitoid emplacement accompanied the Carboniferous evolution of the EMC (Fig. 1). Syn- to post-kinematic plutons and batholiths surround the Velay dome (the "peri-Velay" granites; Faure et al., 2009; Laurent et al., 2017; Ledru et al., 2001). Magmatism migrated southward, beginning within the Forez and Lyonnais areas (North of Saint-Etienne; Fig. 1) at ca. 340 Ma and ceasing in the Cévennes Area (near Alès) at ca. 300 Ma (Laurent et al., 2017). In addition, from ca. 305 Ma to 300 Ma, a large scale thermal event in the central part of the EMC led to the formation of the ~6900 km^2 Velay granite-migmatite dome. Geochemical data indicate that most of the granitoids (including the Velay granite and muscovite- or cordierite-bearing peraluminous granitoids; Fig. 1) derive from melting of metamorphic units. However, this magmatism was spatially and temporally associated with significant input of mantle-derived magmas (e.g., biotite-amphibole calc-alkaline granodiorites, quartz-diorites and high-Mg and high-K mafic rocks; Fig. 1; Barbey et al., 1999, 2015; Couzinié et al., 2014, 2016; Downes et al., 1997; Laurent et al., 2017; Moyen et al., 2016; Solgadi et al., 2007; Williamson et al., 1996; 1997). The formation of the Velay granite-migmatite dome at 310-300 Ma marks the gravitational collapse of the orogen, which was coeval with the development of ductile extensional shear zones and opening of the late Carboniferous (Stephanian) coal-bearing basins (Burg et al., 1990; Burg and Vanderhaeghe, 1993; Malavieille, 1993; Malavieille et al., 1990).

3. The Tournon area – geology and sampling

The Tournon area is located along the eastern border of the Velay dome along the Doux valley a few kilometers from the town of Tournon (Fig. 1). It forms part of a series of N-S

aligned klippen of the UGU that rest atop the LGU, and are dissected by a series of NE-SW-striking dextral strike-slip faults (Gardien, 1993). On the eastern flank of the synformal UGU klippe (Fig. 2), the base of the UGU is characterized by a bimodal association dominated by amphibolite (sample *TN13*) with alternating layers of orthogneisses and minor sillimanite-bearing gneisses (sample *TN21*), a lithological association typical of the LAC. These rocks record MP-MT metamorphism that reached partial melting conditions (as shown by concordant leucosomes), but locally preserves relicts of metabasite boudins and enclaves having been subjected to granulitic and eclogitic conditions (Gardien, 1993). The LAC is structurally overlain by a thick body of two-mica banded gneiss (samples *TN12 and TN07;* Fig. 2) which includes small lenses of sillimanite-biotite gneiss, mostly at its base. The LAC and the base of the two-mica banded gneiss (i.e., close to the contact with the LAC) are crosscut by several generations of peraluminous, K-rich (with biotite ± muscovite) granite dikes generally striking WNW-ESE. A generation of early dikes (samples *TN14 and TN40*) tend to be less foliated than late dikes (samples *TN11* and *TN32*).

On the western flank of the klippe, the UGU is separated from a homogeneous biotite-bearing granite phase (sample *TN01*) of the Velay granite-migmatite complex by a prominent NNW-SSE striking, sub-vertical mylonitic zone (Fig. 2). The more typical, heterogeneous Velay granite (sample *TN09*) is exposed further West in the Doux valley, below migmatitic cordierite-bearing gneisses and augen gneisses (Fig. 2). This heterogeneous granite contains many fragments of country rocks (including an enclave of porphyritic biotite granite dated at 321.9 ± 1.3 Ma; Laurent et al., 2017) and is characterized by the presence of cockade-type cordierite (see Barbey et al., 1999).

The contact between the UGU and the LGU is exposed along the eastern flank of the klippe, where it is transposed into the synmigmatitic foliation. The LGU in this area is made up by mylonitic orthogneisses, migmatitic paragneisses (samples *TN17* and *TN46*) and small

lenses of amphibolite (Fig. 2). The degree of migmatization of the LGU broadly increases toward the east, reflecting an evolution towards lower structural (Fig. 2). Further east, the LGU is intruded by the 321.1 ± 1.1 Ma-old (U-Pb zircon) Tournon porphyritic biotite granite (Laurent et al., 2017) which belongs to the suite of the "peri-Velay" granites (Ledru et al., 2001).

Detailed descriptions and coordinates of all samples investigated are provided within the electronic supplementary material (ESM1).

4. Analytical Methods

Zircon separation was carried out at the University of Geneva. Rock samples were crushed and <400 µm sieved fractions were processed using a Wilfley shaking table, a Frantz magnetic separator and heavy liquids (methylene iodide) to extract zircons. Zircons grains were handpicked under a binocular microscope, mounted in epoxy, cut in half, and polished to expose their interior. In order to obtain the largest variety of grain types and minimize sampling bias, zircons were selected randomly without filtering for inclusion-free, fracture-free, core-free or transparent grains. All grains were subsequently imaged with cathodoluminescence (CL) on a JEOL CamScan scanning electron microscope (using a 10 kV accelerating voltage) at the University of Geneva (Fig. 3).

U-Th-Pb isotopic data were obtained by laser ablation inductively coupled plasma mass spectrometry (LA-ICPMS) at the Laboratoire Magmas et Volcans of Clermont-Ferrand, France, using an Agilent 7500cs ICP-MS equipped with a dual pumping system to enhance sensitivity (Paquette et al., 2014), and interfaced to a Resonetics Resolution M-50 193 nm ArF Excimer laser system. Data were corrected offline for U-Pb fractionation and instrumental mass discrimination. These corrections and the determination of the U-Th concentrations were carried out by normalizing to the GJ-1 zircon standard (Jackson et al.,

2004). The 91500 zircon standard (Wiedenbeck et al., 1995), was used as secondary standard to control the reproducibility and accuracy of the method.

Lu–Hf isotope measurements were performed by laser ablation, multi-collector inductively coupled plasma mass spectrometry (LA-MC-ICPMS) at the Goethe University, Frankfurt am Main (Germany) and the University of Geneva (Switzerland). All spots for Lu–Hf isotope analyses were placed "on top" of previous U–Pb dating spots, or alternatively within the same internal zircon domains as identified in CL images, exclusively where concordant U–Pb dates were obtained. Accuracy and external reproducibility of the method were controlled by repeated analyses of $^{176}Hf/^{177}Hf$ ratios in reference zircon standards GJ-1 (Morel et al., 2008), Plešovice (Sláma et al., 2008), Temora (Woodhead and Hergt, 2005), Mud Tank (Woodhead and Hergt, 2005) and 91500 (Blichert-Toft, 2008)

Details concerning analytical methods, instrument setup, data reduction protocols and results on zircon reference materials for both U-Pb and Lu-Hf used in both laboratories can be found in the electronic supplementary material (ESM 2).

5. Results

In this study, only zircon dates with a concordance level of 98-102% concordance (defined as [$^{206}Pb/^{238}U$ date]/ [$^{207}Pb/^{235}U$ date] × 100) are used for density plots with $^{206}Pb/^{238}U$ dates used for dates younger than 1200 Ma and $^{207}Pb/^{206}Pb$ dates used for older dates. A detailed description of zircon textures, U-Pb, Lu-Hf isotopic data, and Th/U ratios for each sample or group of samples can be found in the electronic supplementary material (ESM 3). These datasets are presented in Figures 3 to 9 and summarized hereafter.

Zircon U-Pb dates from all four samples of the UGU (paragneisses *TN07* and *TN21*, banded gneiss *TN12*, and amphibolite *TN13*) define a prominent population at ca. 480 Ma. Sample *TN13* is characterized by a suprachondritic εHf_t (ca. +9) and homogeneous Th/U (ca.

0.5), while the samples *TN07*, *TN12* and *TN21* have contrasting subchondritic εHf_t (–1 to –10) and scattered Th/U (1-0.05) (Figs. 4, 7, 8). An Ediacaran (ca. 650–550 Ma) zircon population (Fig. 4) is present within each samples (yet better represented within paragneiss samples *TN07* and *TN21*). Zircon within this population are characterized by a restricted range of Th/U (mostly between 1 and 0.2; Fig. 7) and a huge scatter in εHf_t from +8 to –27 (Fig. 8). Samples *TN12* and *TN13* are characterized by an additional ca. 350-340 Ma population of zircon (Fig. 4) with very low Th/U ratios of 0.18-0.003 (Fig. 7) and variable εHf_t, from ca. –5 in *TN12* up to positive values (+1 to +7) in *TN13* (Fig. 8). A few zircons have dates >700 Ma and positive εHf_t.

Altogether, zircons from the two LGU migmatitic paragneisses (*TN17* and *TN46*) and the Velay granites (*TN01* and *TN09*) display (i) a similar population having late Carboniferous dates at ca. 308 Ma (Fig. 5) with highly scattered Th/U ratios (1-0.01; Fig. 7) and subchondritic εHf_t (ca. –5 with outliers down to –15; Fig. 8); and (ii) a zircon gap between ca. 550 and 350 Ma. However, the samples define two groups according to the characteristics of zircons with U-Pb dates >500 Ma. The two Velay granite samples contain a prominent population of zircons with U-Pb dates of ca. 548 Ma (Fig. 5), scattered Th/U ratios centered around 0.1 (Fig. 7) and relatively homogeneous, slightly subchondritic εHf_t (0 to –5; Fig. 8), with only very few older grains. In contrast, the two paragneiss samples contain zircons with dates scattered mostly between ca. 528 and 622 Ma and up to 961 Ma (Fig. 5). The latter group is characterized by a narrow range of Th/U ratios (1-0.2; Fig. 7) but a huge scatter of εHf_t (+8 to –20; Fig. 8), very much like zircons having the same U-Pb dates in the two UGU paragneisses.

Zircon populations from the granite dikes have mixed characteristics from both the UGU and the LGU. They define four main U-Pb date populations: (i) 650-575, (ii) 560-540, (iii) 490-460, and (iv) 325-305 Ma, with few older dates including a 950-1050 Ma group (Fig.

6). All groups have similar Th/U ratios and εHf_t signatures as coeval zircons of the UGU and the LGU samples (Figs. 7, 8), i.e. (i) scattered Th/U and subchondritic εHf_t at 325-305 Ma; (ii) scattered Th/U and εHf_t (from sub- to suprachondritic) at 490-460 Ma; (iii) scattered Th/U and nearly chondritic εHf_t at 560-540 Ma; and (iv) homogeneous Th/U but highly scattered εHf_t at 650-575 Ma.

All samples (with exception of *TN13*) contain zircons dated at older than 1.2 Ga (n = 103 in total; Fig. 9). The few sub-concordant analyses (n = 27) define two clusters at 1.89-2.10 Ga and 2.66-2.84 Ga, corresponding to sub-chondritic εHf_t (–1 to –21 at 1.89-2.10 Ga; 0 to –5 at 2.66-2.84 Ga; Figs. 9, 10). The discordant analyses plot along diffuse Discordia lines between these two clusters and a younger age interval (800-550 Ma; Fig. 9). In addition, four slightly discordant analyses have $^{207}Pb/^{206}Pb$ dates greater than 3.0 Ga (up to 3322 ± 7 Ma).

6. Interpretation of U-Pb dates

6.1. Upper gneiss unit

In the UGU gneisses (*TN07*, *TN12*, *TN21*), the prominent peak of Lower Ordovician dates at ca. 480 Ma was most frequently obtained from zircon rims overgrown on older cores (~70%), and less often from entire grains (~30%; Figs. 3, 4). Furthermore, in contrast to the very scattered Hf isotopic signature of zircons older than 550 Ma (εHf_t of –28 to +10), this Ordovician peak shows a relatively homogeneous Hf isotopic signature (εHf_t of –1 to –7, excluding few outliers; Fig. 8). We interpret those observations as reflecting an important ca. 480 Ma thermal event that resulted in partial melting of the protolith, zircon resorption, and subsequent crystallization of isotopically homogeneous overgrowths. The overgrowths generally have lower Th/U ratios (<0.2) than the older Neoproterozoic cores (>0.2; Fig. 7), which may indicate that zircon recrystallized in presence of a competing phase for Th, such as monazite.

The significant amount of Neoproterozoic zircons (mostly cores), and their large spread of U-Pb dates and Hf isotope compositions (Figs. 7, 8) support a hypothesis of a sedimentary protolith for the UGU gneisses. The depositional age of the sedimentary protoliths is bracketed between the late Ediacaran age of the youngest significant U-Pb date cluster obtained from detrital zircon cores (ca. 555 Ma), and the lowermost Ordovician, i.e. before the ca. 480 Ma thermal event. Single dates between these two peaks are likely to be reflective of Concordia-parallel Pb loss.

By contrast, in the amphibolite *TN13*, the Lower Ordovician dates were almost exclusively obtained from zircon cores (Concordia age of 486.4 ± 3.1 Ma; Fig. 4). Moreover, these Ordovician zircons have distinct chemical and isotopic signatures with respect to their counterparts in the gneisses (Figs. 7, 8); they show homogeneous and positive εHf_t values, close to the composition of the depleted mantle (average εHf_t = +8.9 ± 1.5; n = 19), and very homogeneous, typically magmatic Th/U ratios (0.23-0.47). We therefore interpret the Ordovician zircon population in the amphibolite as reflecting the emplacement age of the mafic magmatic protolith. This was presumably part of the same ca. 480 Ma event responsible for the thermal overprint recorded by zircons in the host UGU metasediments.

In addition to the ca. 480 Ma rims, zircons from the banded gneiss (*TN12*) commonly display a thin outer rim characterized by a U-Pb Concordia date of 351.5 ± 3.0 Ma (Figs. 3, 4). Similarly, zircon from the amphibolite (*TN13*) with ca. 480 Ma cores frequently exhibit zircons rims with a U-Pb Concordia date of 343.5 ± 2.6 Ma (Figs. 3, 4). In both samples, these early Carboniferous rims clearly display much lower Th/U ratio (most often <0.05; down to 0.002) compared with the cores (0.05–1; Fig. 7). This observation is commonly considered characteristic of metamorphic zircon where recrystallization purges Th and Pb from the crystal lattice in the metamorphic domains, resulting in low Th/U rim and resetting of the U-Pb system (e.g., Hoskin and Schaltegger, 2003). In the banded gneiss (*TN12*), the

$^{176}Hf/^{177}Hf_t$ of these metamorphic zircon rims connect with their magmatic ca. 480 Ma cores along a trend characterized by $^{176}Lu/^{177}Hf \sim 0.015$ (Fig. 11), consistent with an average crustal composition and thus, with the expected clastic sedimentary protolith of sample *TN12* (see above). Collectively, these results suggest that these zircon rims result from incipient partial melting of the gneiss, under near-solidus temperature conditions where the Th/U zircon/melt distribution coefficient is dramatically reduced owing to temperature-dependent lattice-strain partitioning constrains (Blundy and Wood, 1994). In contrast, $^{176}Hf/^{177}Hf_t$ ratios of the metamorphic rims in the amphibolite (*TN13*) plot at significantly lower values than what would be expected from pure metamorphic zircon alteration (Fig. 11), i.e. U-Pb age re-equilibration without changing the Hf isotopic composition (Amelin et al., 2000; Gerdes and Zeh, 2009; Lenting et al., 2010). This necessarily requires that some amount of non-radiogenic Hf was added to the system during the metamorphic event, and incorporated in the newly crystallized zircon rims. A fluid or melt phase derived from the surrounding UGU gneisses would represent a plausible source of such non-radiogenic Hf because those gneisses, as indicated by sample *TN12*, show a much lower $^{176}Hf/^{177}Hf_t$ than the amphibolite at the time of this metamorphic overprint (Fig. 11).

In summary, zircon U-Pb and Lu-Hf data support the interpretation that the youngest zircon rims in samples *TN12* and *TN13* formed by incipient dissolution/recrystallization of the original (detrital or magmatic) zircon, with subordinate Hf mobility possibly promoted by a coeval melt or fluid phase during an Upper Devonian to early Carboniferous (Variscan) migmatitic-metamorphic episode.

6.2. Lower gneiss unit

In the two migmatitic paragneisses (*TN17* and *TN46*), zircons with concordant dates ranging from the Neoproterozoic (ca. 530 Ma) to the Mesoarchean, display scattered εHf_t (–20 to

+8), and relatively homogeneous Th/U ratios from 0.2 to 1 (Figs. 7, 8). These characteristics are very similar to those of detrital zircons in the UGU gneisses. This is consistent with a similar sedimentary protolith for both LGU and UGU gneisses, of which the maximum depositional age likely corresponds to that of the youngest Ediacaran peak at ca. 554 Ma. We also note that within the Velay area, the LGU paragneisses are intruded by ca. 540-545 Ma granites (now augen orthogneisses, see below; Mintrone 2015). It brackets the depositional age of the sedimentary protolith of the LGU paragneisses to the latest Ediacaran (550-555 Ma). By comparison, a similar age may be envisioned for the protolith of the UGU paragneisses although deposition during the Cambrian cannot be totally excluded.

In the Velay granites (*TN01* and *TN09*), inherited zircons are strikingly dominated by a 550-545 Ma-aged population (Fig. 5). Compared with zircons showing the same U-Pb dates in the paragneisses, these grains show a more homogeneous Hf isotope composition (most concordant data at ca. 550 Ma have εHf_t between –0.5 and –2.5; Fig. 8) and lower Th/U ratios (Fig. 7). This suggests that they have a different origin and may derive from a single igneous unit emplaced between 550.2 ± 3.1 Ma (*TN01*) and 544.3 ± 3.1 Ma (*TN09*), possibly represented by the migmatitic augen orthogneisses (not dated) located NW of the study area (Fig. 2). This assumption is supported by the fact that most orthogneisses of the LGU in the Velay area belong to a former, widespread S-type granitic batholith emplaced in the late Ediacaran at ca. 545 Ma (Mintrone, 2015; R'Kha Chaham et al., 1990). The broad and generally low Th/U values (0.02–1) of the ca. 550 Ma zircons from the Velay granite (Fig. 7) suggest that they co-crystallized with a Th-rich accessory mineral such as monazite. Such monazite is documented in peraluminous orthogneisses from the southern Velay dome (Be Mezeme et al., 2006) and as inherited grains (with an age of ca. 540 Ma) within the microgranites associated with the Velay granite (Didier et al., 2013).

In samples *TN01* and *TN09*, few zircons cores overgrown by ca. 550 Ma rims have a large spread of both Neoproterozoic U-Pb dates and ε Hf_t (–20 to +8), and more restricted Th/U ratios (2.5 to 0.3), all of which overlap with those from the detrital zircons of the paragneisses (Figs. 7, 8). Therefore, we interpret these older zircons either as (i) inherited from the source of the 550 Ma granites which may be comparable to the LGU paragneisses (maybe slightly older), (ii) assimilated from the LGU paragneisses upon emplacement of the 550 Ma granites or during the formation of the Velay granite, or (iii) a combination thereof. However, it is noteworthy that at least some of the ca. 550 Ma zircons with Th/U ratio over 0.2 and ε Hf_t between –0.5 and –2.5 (i.e., belonging to the main inherited population in the Velay granite) might be of detrital origin (assimilated or inherited) and cannot individually be discriminated from those magmatic zircons having similar Th/U and ε Hf_t.

In the Velay granites, a few entire grains with oscillatory zoning or thin rims overgrown on older cores record Carboniferous dates (309 ± 2.6 Ma for *TN01* and 307.5 ± 2.0 Ma for *TN09*; Figs. 3, 5), interpreted as the age of crystallization of the Velay granite at Tournon. These ages are consistent with other geochronological data obtained from the Velay granites-migmatites, all yielding ages in the range 300–310 Ma (Couzinié et al., 2014; Didier et al., 2013; Laurent et al., 2017; Mougeot et al., 1997). In the LGU migmatitic paragneiss *TN17*, the age of the migmatization is well recorded by zircon rims on older cores or entire grains (307.4 ± 2.3 Ma) and overlap within uncertainty with the age of the Velay granite as dated on *TN01* and *TN09* (Fig. 5). This event is, in contrast, poorly recorded in sample *TN46* (only 2 concordant analyses around 310 Ma), which is consistent with its apparent lower degree of partial melting.

In the LGU, the few concordant analyses with dates ranging from ca. 310 to 540 Ma most probably represent lead loss of the ≥540 Ma-old zircons (Fig. 5) during Variscan events (which would still result in concordant analysis within the analytical precision). This

interpretation is supported by the fact that these zircons were exclusively found in the two Velay granite samples (*TN01* and *TN09*), where partial resetting of the U–Pb system in inherited zircons is likely to have taken place owing to dissolution/recrystallization, whereas zircons dates from the two LGU paragneisses samples (*TN17* and *TN46*) clearly show a complete gap between ca. 550 and 320 Ma (Fig. 5).

6.3. Granite dikes

All four granite dikes samples show a group of Carboniferous zircon rims and entire oscillatory-zoned grains that have been used to calculate U-Pb dates ranging from 323.3 ± 3.5 Ma (*TN14*) to 307.9 ± 3.3 Ma (*TN32*; Figs. 3, 6). These dates are fully consistent with cross-cutting relationships and furthermore overlap with ages recently obtained on Variscan granitoids in the eastern FMC (340–300 Ma; Laurent et al., 2017). Therefore, these dates are considered to represent the emplacement ages of the dikes.

All samples further show a range of older zircon, mainly >470 Ma with scattered εHf_t from –18 to +12 and predominantly obtained from zircon cores (Fig. 8), which would correspond to either inherited grains from the source, or zircon sampled from wall rock during magma ascent and emplacement. Few grains dated at ca. 480 Ma display positive εHf_t comparable to those from the crosscut amphibolite (sample *TN13*) while others with εHf_t between 0 and –5 are akin to those from the UGU gneisses (Fig. 8). Most zircons dated at ca. 550 Ma display chondritic Hf isotopes and very scattered Th/U (0.2 to 2), similar to inherited zircons from the Velay granites (Figs. 7, 8). Finally, Ediacaran and older zircons (>550 Ma) display U-Pb, Th/U and εHf_t characteristics similar to detrital zircons from the UGU and the LGU (Figs. 7, 8). These elements suggest that inherited and/or xenocrystic zircons from the granite dikes are of various magmatic and detrital origins and have been sourced from both the UGU and the LGU. This pattern of ages and isotopic compositions of inherited zircons is

also notably similar to that observed from other Variscan granitoids in the area (Couzinié et al., 2014; Laurent et al., 2017; Moyen et al., 2016).

7. Discussion

7.1. Paleogeographic position

The terranes involved in the European Variscides are commonly interpreted as derived from the northern margin of Gondwana (Garfunkel, 2015; Henderson et al., 2015; Kroner and Romer, 2013; Matte, 2001; Nance and Murphy, 1994; Zeh et al., 2001; Zeh and Gerdes, 2010). This interpretation is supported (1) by sedimentologic, paleontogical and paleomagnetic data indicating a common south polar position of all these terranes (Cocks and Torsvik, 2002; Fortey and Cocks, 2003; Paris and Robardet, 1990; Robardet et al., 1990; Tait et al., 2000; 1997), and (2) by detrital zircons from late Proterozoic to early Paleozoic metasediments sampled throughout the European Variscides characterized by a predominance of ages related to the Pan-African orogenies (that resulted in the amalgamation of Gondawana; 0.55–0.70 Ga) and the African cratons (1.9–2.1 Ga and 2.7–3.3 Ga) with a characteristic gap between ca. 1.2 and 1.7 Ga (e.g., Drost et al., 2011; Fernández-Suárez and Gutiérrez-Alonso, 2000; Gebauer et al., 1989; Gerdes and Zeh, 2006; Keay and Lister, 2002; Linnemann et al., 2014; Melleton et al., 2010; Shaw et al., 2014; Sirevaag et al., 2016; Zeh and Gerdes, 2010).

This characteristically North Gondwanan signature is obvious in the repartition of zircon ages obtained from the Tournon area (Fig. 9). The Stenian-Tonian ages (ca. 1050-950 Ma) can be attributed to the assembly of the Rodinia supercontinent during the Grenvillian orogenies (Bradley, 2011; Rino et al., 2008), while ages of 700 to 550 Ma correspond to the assembly of Gondwana during several (Pan-African) collisional orogenies, and by the formation of an Andean-type orogenic belt along its northern margin during the Ediacaran,

the Cadomian-Avalonian belt (Bradley, 2011; Linnemann et al., 2008; Nance and Murphy, 1994; Rino et al., 2008; Veevers, 2004). Extensional rifting of the northern Gondwana margin during the early Paleozoic is recorded by the ca. 480 Ma age peak. This event resulted in the opening of the Rheic Ocean and probably other smaller oceanic domains (e.g., Galicia-Massif Central Ocean(s)), and the drift of the Avalonian continental ribbon away from the main Gondwana supercontinent (e.g., Gerdes and Zeh, 2006; Linnemann et al., 2008; Nance et al., 2010; Ballèvre et al., 2014). Finally, the closure of these oceans from the Devonian to the Carboniferous led to the formation of the supercontinent Pangea during the Variscan orogeny (e.g., Kroner and Romer, 2013; Matte, 2001, Nance et al., 2010), as is partly recorded by the ca. 360-300 Ma date cluster in the Tournon area (Fig. 9).

Although the general tectonic evolution of the Gondwana supercontinent is considered to be well-established, there are still uncertainties concerning the lateral positions occupied by individual Gondwana-derived Variscan terranes along the northern Gondwana margin during the late Neoproterozoic and early Paleozoic. Published models from the Massif Central range from a paleogeographic position adjacent to the West African craton (e.g., Henderson et al., 2015; Linnemann et al., 2004; Samson et al., 2005) to a position adjacent to the Arabian-Nubian Shield (e.g., Keppie et al., 2003; Murphy et al., 2006; Stampfli et al., 2013). Here we compare the detrital zircon record (U-Pb ages and Hf isotopes) from the Tournon area (considering all grains >580 Ma-old) with available zircon data from non-metamorphosed Cambro-Ordovician sandstones across North Africa (from Morocco to Jordan; Figs. 10, 12). Although these sediments might not be of the exact same age as those from Tournon (deposited during the late Ediacaran-Cambrian), they can still provide important information about the characteristics of their respective source catchment basins in the Gondwana hinterland, to be compared with the age spectra from the Tournon area. The legitimacy of the comparison is also supported by the observation that late Ediacaran metasedimentary rocks in

the Iberian massif (interpreted to have been deposited in a back-arc setting) have detrital zircon signatures very similar to those within Ordovician sediments (interpreted to have deposited in a passive margin setting; see Shaw et al., 2014). Distinct isotopic signatures between the North African sediments and their local basement, together with northward paleocurrent directions were interpreted to reflect long-distance sediment transport (several 1000s of km, presumably assisted by glaciers) from hinterland Gondwana massifs located to the south such as a Transgondwanan Supermountain (separating East and West Gondwana) and deposition in a continental-scale 'super-fan' (Avigad et al., 2012; Meinhold et al., 2013; Morag et al., 2011a; Squire et al., 2006).

Non-metric multi-dimensional scaling analysis (Fig. 12b; Vermeesch, 2013) show that Israeli and Moroccan zircons are the closest neighbors to those from the EMC. Additional visual comparison of the age spectra (Fig. 12a) suggests that the zircon population from Tournon is much more akin to the one of the Israeli sediments because:

- sediments from Morocco lack the Meso-Neoarchean zircon age peak seen in Tournon
- the ca. 660 Ma age peak characteristic of Morocco corresponds to a trough in the Tournon samples
- detrital zircons from Tournon present individual Pan-African peaks (710, 625 and 590) that are best matching the sandstones from Israel.

Furthermore, Paleoproterozoic zircons (2.1-1.9 Ga) in sediments from Morocco show a predominant juvenile Hf isotope signature (Abati et al., 2012; Avigad et al., 2012) (Fig. 10), similar to that of exposed magmatic rocks from the Eburnean/Birimian belts of the West African craton (Block et al., 2016) but not observed in the Tournon (meta)sediments, in which the Paleoproterozoic zircons have negative εHf_t (Fig. 10). In contrast, Paleoproterozoic zircons from the Israeli sediments have negative εHf_t similar to those from Tournon (Morag et al., 2011a), which clearly suggests that pre-Cadomian detritus of the EMC were not derived

from the West African craton, but rather from the same massifs that sourced the Israeli sediments. Most Neoproterozoic (800-650 Ma) detrital zircons from the EMC show superchondritic εHf_t values overlapping with those from Neoproterozoic clastic and magmatic rocks from the Arabian-Nubian Shield (Fig. 10; Morag et al., 2011b; 2012; Avigad et al., 2015). However, the Arabian-Nubian Shield cannot be considered as the only source of detritus for the EMC Ediacarian sediments, because 67% of the 580-650 Ma detrital zircons from the latter have clearly less radiogenic Hf isotopic compositions (εHf_t from 0 to –28; Fig. 10). This indicates that the Tournon detritus were also fed by exposed granitoid rocks that formed by significant reworking of Meso-Paleoproterozoic and Archean rocks during the Pan-African orogenies. Therefore, areas that are characterized by marginal reworking of ancient cratonic crust comparable (but not necessarily identical) to the West African or Congo cratons (or their erosional products), such as a Transgondwanan Supermountain (Meinhold et al., 2013; Squire et al. 2006), or potentially the southern side of the Saharan metacraton (in which most igneous rocks have Nd model ages >1.5 Ga and up to 3.1 Ga; see Abdelsalam et al., 2012 and references therein) represent more plausible sources.

Altogether, U-Pb and Hf data suggest that during the late Ediacaran-Cambrian period, the EMC block was most likely located in the vicinity the Arabian-Nubian shield and the Saharan metacraton, which is consistent with (i) the most recent reconstruction of Stampfli et al. (2013) and (ii) the close location of the Massif Central with respect to the Iberian Massif, which was previously interpreted as derived from linear ribbon that stretched the length from the Saharan metacraton to the Arabian-Nubian shield during the lower Paleozoic (Orejana et al., 2015; Pastor-Galán et al., 2013; Shaw et al., 2014).

7.2. Pre-Variscan evolution of the north Gondwana margin in the EMC

The age spectra and Hf isotopic data of zircons in the samples from the LGU and UGU show characteristic differences, which point to a different timing of pre-Variscan formation (Figs. 7, 8). The most prominent differences are that (i) samples from the UGU show evidence for an important episode of early Ordovician mafic magmatism and crustal partial melting at ca. 480 Ma (see §6.1) that is totally absent in samples from the LGU; and (ii) samples from the LGU (especially the Velay granites) record a major Ediacaran (ca. 550 Ma) magmatic episode (now represented by widespread orthogneisses in the LGU; see §6.2) that is hardly represented in the UGU. Despite this, the >550 Ma-old detrital zircons in metasediments from both units are characterized by the same ages, Th/U and Hf isotopic characteristics (Figs. 7, 8). Therefore, it appears that the paragneisses of the UGU and the LGU in the EMC most likely represent the same late Ediacaran sedimentary sequence that is distinguished by contrasted pre-Variscan magmatic-metamorphic record, in addition to distinct Variscan metamorphic histories. The characteristics of this pre-Variscan record are further addressed in the following.

The late Ediacaran magmatism strikingly dominates the inherited zircon record of the Velay granites *TN01* and *TN09* (Fig. 5) and is also most likely represented by the migmatitic augen orthogneiss present NW of the study area. Similar orthogneisses, locally migmatitic and exposed all around the Velay dome have been dated around the Ediacaran-Cambrian boundary (ca. 530–550 Ma) which confirms that they represent a widespread, self-consistent unit (Be Mezeme et al., 2006; Caen-Vachette, 1979; Mintrone, 2015; Montel et al., 1992; R'Kha Charam et al., 1993; Weisbrod et al., 1980). Elsewhere in the western and southern sides of the Massif Central (Limousin, Montagne Noire), various orthogneisses yielded similar Ediacaran to Cambrian ages (Alexandre, 2007; Alexandrov et al., 2001; Duthou et al., 1984 and references therein, Lafon, 1984; Lévêque, 1985; Melleton et al., 2010).

The geodynamic significance of this important late Ediacaran to early Cambrian granitoid formation remains poorly constrained in the EMC. It is generally accepted that during the late Neoproterozoic exotic terranes were accreted to the North Gondwana margin to form the Cadomian domain (see Garfunkel, 2015 and references therein). In the European Variscides, most of the Cadomian outcrops actually record only the latest Ediacaran period and are made of a thick siliciclastic marine sedimentary pile derived from both the Gondwana hinterland and from local magmatic sources (e.g., a Cadomian magmatic arc; Garfunkel, 2015). Only few segments of the Cadomian domain keep record of a late Ediacaran magmatic arc and orogenic event (Garfunkel, 2015). In turn, the Ediacaran record is dominated by wide basinal areas that were intruded by voluminous granitoids and usually record limited sub-contemporaneous deformation (Abbo et al., 2015; Garfunkel, 2015 and references therein). In many places, of which domains now adjacent to the EMC such as the Maures Massif and the eastern Pyrenees, the lack of a significant Cadomian-aged deformation, and the presence of bimodal magmatism with mantle (suprasubduction tholeiitic to calc-alkaline metabasite) and crustal (peraluminous metavolcanics/metagranitoids) affinities dated at ca. 560-540 Ma suggest that a large part of the Cadomian domain was undergoing crustal stretching (e.g., Bellot et al., 2010; Castiñeiras et al., 2008; Garfunkel, 2015; Innocent et al., 2003).

Collectively these data are consistent with the emplacement of a widespread ca. 550 Ma-old granitic pluton or batholith within a large, late Ediacaran sedimentary sequence and is now mostly involved into Velay dome. It possibly originated from crustal melting triggered by the incipient inversion of an Ediacaran back-arc basin (Mintrone, 2015). Nevertheless, the relation of these late-Ediacaran granite intrusions in the EMC to a possible subduction zone along the northern border of the same crustal block remains unclear and structural evidence for basin inversion has not been described thus far. In any case, it must be noted that these late Ediacaran meta-sedimentary and meta-igneous units do represent the oldest protoliths

identified within the EMC to date. Indeed, all zircons older than ca. 550 Ma in the Tournon samples arguably correspond to detrital zircons within paragneisses of the UGU and LGU (see §6).

The time interval between ca. 540-490 Ma is marked by an apparent gap in the zircon record of the Tournon area (Fig. 9), unlike in the adjacent massifs (e.g., the Alpine massifs (von Raumer et al., 2013 and references therein); Limousin (Melleton et al., 2010 and references therein); Vosges (Skrzypek et al., 2014 and references therein), Montagne Noire (Faure et al., 2010)). We propose that during the Cambrian, a stable continental platform was established in at least part of the future EMC and that continued tectonics and related magmatic activity (e.g., von Raumer and Stampfli, 2008) was rather focused in peripheral areas.

After this magmatic lull, zircons from the UGU testify that enhanced thermal regime and bimodal magmatic activity resumed around 480 Ma (Figs. 4, 8), which is the age of mafic magma emplacement (protolith of the amphibolite *TN13*) and of partial melting in the Ediacaran (meta)sediments (recorded in the UGU gneisses). This bimodal magmatism is best explained in a context of a thermal event caused by crustal extension, thinning and eventually rifting.

Throughout Europe, such a Lower Ordovician bimodal magmatism is very well represented. A wealth of evidence shows that during this period, the Avalonian terranes drifted from northwest Gondwana, which caused the diachronic west to east opening of the Rheic ocean (e.g., Linnemann et al., 2008; Nance et al., 2010; von Raumer and Stampfli, 2008). Nevertheless, the Rheic suture zone is now recognized in southern England and south of the Rhenish Massif, while south of this suture, many relicts of mafic-ultramafic complexes, MORB-type eclogites, alkalic magmas and contemporaneous crust-derived acidic magmatic rocks of Upper Cambrian-Lower Ordovician ages are found (see compilations in: Berger et

al., 2006; von Raumer et al., 2013; 2015; Villaseca et al., 2015). Despite some disagreement about the source and geodynamic implication of such magmatism, it is generally agreed that at this period the northern Gondwana margin was under widespread extensional tectonics that locally led to the formation of slow-spreading oceanic crust, distinct from that of the Rheic Ocean (Berger et al., 2006; Bouchardon et al., 1989; Briand et al., 1991; Díez Fernández et al., 2012; Matte, 2001; Montes et al., 2010; Pin and Marini, 1993; von Raumer and Stampfli, 2008). In the Massif Central, this "oceanic" domain is often referred to as the Galicia-Brittany Ocean (Matte, 2001) or Massif Central-Moldanubian Ocean (Tait et al., 1997). However, the continuity of the benthic faunas and paleomagnetic data preclude the existence of a large ocean between the Massif Central and Gondwana during the Ordovician and the Silurian (Cocks and Torsvik, 2002; Fortey and Cocks, 2003; Paris and Robardet, 1990; Shaw and Johnston, 2016; Tait et al., 2000). Accordingly, an Ocean-Continent transition (Lardeaux et al., 2014) or an hyperextended north Gondwana margin would represent more realistic settings for the Ordovician period.

7.3. Timeframe of Variscan events in the EMC

The new U-Pb and Lu-Hf isotopic data from zircons of the Tournon area record several Carboniferous metamorphic and magmatic events and thus place new constraints on the Variscan evolution of the EMC.

The data indicate that zircon grains/overgrowths in the banded gneiss (*TN12*) and the amphibolite (*TN13*) from the UGU (Figs. 7, 8) were formed during a migmatitic-metamorphic event at around 350-340 Ma (see §6.1 and Fig. 11). The lack of HP assemblage within the migmatitic portions of sample *TN12* and *TN13* shows that these ages unlikely reflect the timing of HT-HP metamorphism of the UGU (up to ca. 800°C, 15 kbar; Gardien, 1993).

Instead we argue that these correspond to incipient anatexis and crystallization of the nappe on the retrograde path to amphibolite facies conditions.

Our early Carboniferous metamorphic ages for the LAC of Tournon are similar to a zircon ID-TIMS U-Pb age 345 ± 10 Ma in the Marvejols area (south Massif Central) where a bimodal series resembling that of Tournon records retrograde (after HP) amphibolite facies metamorphism (Pin and Lancelot, 1982). Our new data further suggest that in the southern part of the Massif Central the retrogression of the UGU to amphibolite facies conditions (Gardien, 1993) in association with incipient partial melting occurred significantly later (ca. 350-340 Ma) that in the northern part (389-375 Ma; Boutin and Montigny, 1993; Costa and Maluski, 1988; Duthou et al., 1994). This implies that rocks forming the UGU in the southern Massif Central were buried and exhumed later than in the northern Massif Central and/or that after syn-orogenic exhumation to mid-crustal depth, they remained partially molten for a longer time period.

The base of the UGU was later affected by intense magmatic activity with several generations of granite dikes emplaced from 323.3 ± 3.5 Ma (*TN14*) to 307.9 ± 3.3 Ma (*TN32*; Fig. 6). This timing of dike intrusion overlaps with the emplacement of numerous peri-Velay granite plutons, including the nearby Tournon granite (Fig. 2) dated at 321.1 ± 1.1 Ma (see *TN19* in Laurent et al., 2017). It is noteworthy that the U-Pb, εHf_t, and Th/U characteristics of inherited and/or xenocrystic zircons in these dikes overlap with those obtained from both the UGU and LGU rocks (Figs. 7, 8; including signatures of LGU paragneisses, LGU-derived Velay granite, UGU gneisses and UGU amphibolite). This suggests that the dikes were formed either by partial melting of rocks from both units, and/or by melting of the LGU rocks with subsequent assimilation of the UGU lithologies during emplacement. The observation that migmatitic leucosomes of the LAC lithologies are locally in textural continuity with some of the granite dikes favors the first hypothesis. In either case, this indicates that stacking of

the UGU nappe above the LGU must have been achieved by ca. 325 Ma, that is, prior to the emplacement of the oldest dikes.

The youngest dike (*TN32*; 307.9 ± 3.3 Ma) is concomitant with the emplacement of the Velay granites, dated at 309.6 ± 2.9 Ma (*TN01*) and 307.5 ± 2.0 Ma (*TN09*) in Tournon and in the 310–300 Ma time span elsewhere in the EMC (Couzinié et al., 2014; Didier et al., 2013; Laurent et al., 2017; Mougeot et al., 1997). Overall, data from the dikes argue for the presence of a 15.4 ± 4.8 Ma-long lasting thermal anomaly in the Tournon area, accompanied with protracted crustal partial melting and granite dike intrusion. The exhumation of the Velay dome marks the end of this high crustal thermal regime and suggests that the existence of a long-lived molten zone in the middle crust possibly controlled dome extrusion and gravitational collapse (Ledru et al., 2001; Vanderhaeghe, 2009; Vanderhaeghe and Teyssier, 2001). The nearly continuous intrusion of high-K mantle-derived magmas between 335 and 300 Ma in the EMC, provides a clue that protracted crustal melting was concomitant with asthenospheric mantle upwelling caused by late-orogenic lithosphere delamination (Laurent et al., 2017).

7.4. Constraints on crustal growth and recycling

The U-Pb vs εHf_t data from the Tournon area (Fig. 10) suggest that the EMC crust result from the reworking of several juvenile crustal components throughout the geological history. Below we describe the age and origin of these crustal components and their respective reworking associated with each zircon date group from the Tournon area.

Detrital zircons with Archean (3.3-2.5 Ga; n = 8) and Paleoproterozoic ages (2.1-1.9 Ga; n = 14) show dominantly negative εHf_t values from ca. 0 to –20 (Fig. 10), indicating that they crystallized from magmas formed by reworking of pre-existing crust. Hafnium model ages of the zircons with the most negative εHf_t (–10 to –20) indicate that the oldest reworked

crust has been extracted from a depleted mantle source at 3.4–3.1 Ga. These model ages are comparable to those obtained during previous studies from basement rocks of the West African and Congo cratons (Eglinger et al., 2016; Batumike et al., 2009; Potrel et al., 1996; 1998; Tchameni et al., 2001; Fig. 10). Variable εHf_t values (from 0 to –10) of some Paleoproterozoic zircons (2.1-1.9 Ga) may be explained by the interactions between Archean crust (3.0-2.6 Ga) and juvenile magmas during the "Birimian" or "Eburnean" orogenies. This interpretation may be supported by the dominantly positive εHf_t of 2.25-2.05 Ga-old zircons from clastic sediments and magmatic rocks of the West African Craton (Fig. 10; Block et al., 2016; Parra-Avila et al., 2016). Despite their similarities with zircons from the West African and Congo cratons, the magmatic source of the Archean to Paleoproterozoic zircon grains of Tournon is unknown. In fact, the Pan-African rocks that sourced the Ediacaran sediments of Tournon probably already hosted some components derived from the West African, Congo and/or other cratons (see below).

Zircon grains with ages of 1030-850 Ma (n = 12) from the EMC show mostly negative εHf_t, providing evidence for the reworking of Paleoproterozoic to Archean crust of the Gondwana realm during the Grenvillian orogenies (Fig. 10). Similar signatures are also present in detrital zircons from the Cambrian-Ordovician sandstones in Israel and Jordan (Fig. 10; Morag et al., 2011a), but also from minor zircon populations in Saxothuringian sediments in Central Germany (Zeh et al., 2001; Gerdes and Zeh, 2006; Linnemann et al. 2008, 2014) and from the Iberian Massif, Spain and Portugal (Orejana et al., 2015; Teixeira et al., 2011).

Most zircons from Tournon that crystallized in the 800-650 Ma time span show positive εHf_t up to +11 (81%), thus pointing to a period of significant juvenile crust formation (Fig. 10). Similar age-Hf isotope signature are consistently reported from basement rocks of the Arabian-Nubian Shield (Fig. 10; Morag et al., 2011b), and from some Gondwana-derived sediments in Europe (Avigad, 2012; Linnemann et al., 2008; Orejana et al., 2015). This

observation together with the Ediacaran paleogeographic position of the EMC (see §7.1), suggests that a crustal component similar in age and Hf isotopic composition to the rocks of the Arabian-Nubian Shield may have contributed to build the EMC crust.

The εHf_t of zircons crystallized in the time span 650–550 Ma are characterized by an enormous spread of nearly 40 εHf units, from εHf = +11 to –28 (Fig. 10). Such a spread was already described from detrital zircons in various peri-Gondwanian terranes (e.g., Albert et al., 2015; Avigad et al., 2012; Bahlburg et al., 2010; Linnemann et al., 2014; Morag et al., 2011a; Teixeira et al., 2011) and is interpreted to reflect mixing between juvenile Neoproterozoic magmas and ancient (Paleoproterozoic-Archean) Gondwana crust. Linnemann et al. (2014) proposed that the geotectonic setting required to explain such mixing was a continental magmatic arc developed on stretched Archean-Paleproterozoic crust. Alternatively, this large spread of εHf_t may be explained as a sedimentary mixture (deposited during the late Neoproterozoic along the northern Gondwana margin) of which detritus were derived from different crustal regions of the Cadomian/Pan-African orogens, in which magmatism was characterized by various proportions of respectively Archean/Paleoproterozoic, and juvenile Neoproterozoic crustal sources (Morag et al., 2011a). This option is preferred for the EMC as there is so far no compelling evidence for autochthonous crust older than ca. 550 Ma in the EMC (Mintrone, 2015; this study), further supporting the distal origin and the detrital nature of these zircons. Nevertheless, this does not rule out the possible co-existence of Paleoproterozoic crust and Neoproterozoic subduction-related magmatism, similar to that reported is some areas of the Cadomian orogen (e.g., in northern Brittany: Ballèvre et al., 2001; Tauride block: Abbo et al., 2015).

Many zircons of the ca. 550 Ma-old population show a very limited spread in εHf_t from 0 to –5, especially those from the Velay granites in the LGU, which we interpret as inherited from a Cadomian (meta)granitic batholith (see §6.2 and Mintrone, 2015; R'Kha

Chaham et al., 1990). The slightly sub-chondritic Hf isotope signature of zircons from these magmas is rather consistent with a source represented by a relatively homogeneous mixture of juvenile Neoproterozoic and Archean to Paleoproterozoic crustal material. Such a source is possibly represented by the UGU and LGU paragneisses which, as discussed earlier, were fed by mixed detritus from these two crustal components (Figs. 8, 10).

Apart from a minor juvenile input recorded by the emplacement of the amphibolite *TN13* at ca. 480 Ma (average εHf_t of ca. +9), the magmatic episodes at ca. 480 and 340–300 Ma are characterized by zircons having a relatively homogeneous and sub-chondritic Hf isotope composition (most values are from –1 and –7; Figs. 8, 10). These data sit along an average crustal evolution trend together with those from the 550 Ma-old zircons, corresponding to Hf model ages comprised between 1.0 and 1.5 Ga, in agreement with Hf and Nd isotope data from the FMC granitoids (Moyen et al., 2016; Pin and Duthou, 1990; Turpin et al., 1990). Such model ages clearly have no geological significance as zircon in all Gondwana derived sediments throughout Europe provide no evidence for magmatism during this period (Balintoni et al., 2014; Díez Fernández et al., 2012; 2010; Drost et al., 2011; Gebauer et al., 1989; Gerdes and Zeh, 2006; Linnemann et al., 2014; Morag et al., 2011a; Pastor-Galán et al., 2013; Pereira et al., 2012a; 2012b; Shaw et al., 2014; Sirevaag et al., 2016; Villaseca et al., 2016; Williams et al., 2012; Zeh and Gerdes, 2010). Instead, this Hf isotope signature would correspond again to a mixed source consisting of Neoproterozoic (0.6-0.8 Ga), juvenile crust and Archean/Paleoproterozoic crust (2.0-3.3 Ga). Mixing took place during the Cadomian/Pan-African orogenies, through magmatism and mechanical mixing of detritus from various parts of the orogenies.

As a whole, the U-Pb ages and Hf isotope pattern observed in magmatic, metamorphic and detrital zircons from the Tournon area supports (i) the peri-Gondwanian ancestry of the Massif Central, (ii) that juvenile crustal formation in the Gondwanian realm took place during

three episodes in the Meso-/Paleoarchean (3.0-3.5 Ga), Paleoproterozoic (2.1-2.3 Ga) and Neoproterozoic (0.6-0.8 Ga); and (iii) that the crust of the EMC, and possibly large portions of the Western European crust as well, derive from a mixture of these three components as a result of tectono-magmatic and sedimentary processes that occurred during the Cadomian/Pan-African orogenies.

8. Conclusion

Despite its small size (approximately 6×6 km^2, Fig. 2), the Tournon area presents a remarkable record of the evolution of the West European crust from the late Ediacaran to the end of the Carboniferous and bear some information of the Pan-African orogenies. The identification of detrital, magmatic and metamorphic zircons in metamorphic rocks and granites from Tournon together with their Hf isotopic signature allows us to place constrains on the timing and geodynamic significance of sedimentary, magmatic and metamorphic episodes within this time interval (Fig. 13) and lead to the following conclusions:

1. The (meta)sedimentary rocks of both the UGU and LGU from the Tournon area were deposited in a basin located along the northern Gondwanan margin at ca. 550 Ma, specifically in a paleogeographic position close to the Arabian-Nubian shield and/or the Saharan metacraton
2. This basin was developed on unknown preexisting crust. In fact, our data provide no evidence for the existence of an autochthonous crust before the latest Ediacaran (ca. 550 Ma)
3. At ca. 550-545 Ma, the (meta)sedimentary rocks of the LGU underwent substantial melting, either during crustal stretching or back-arc inversion, resulting in the formation of Cadomian “S-type” granites. These granites were later transformed into widespread

augen orthogneisses during the Variscan orogeny, and possibly became a main source of the late-Variscan granites, including the ca. 308 Ma Velay granite-migmatite dome.

4. Zircons from the UGU provide evidence for a main thermal event and bimodal magmatism at 480 Ma, related to an Early Ordovician rifting that led to the opening of an epicontinental oceanic basin (Fig. 13). Mafic, depleted mantle-derived magmas (now amphibolites) coexisted with partial melting of the Ediacarian (meta)sediments.
5. The scarcity of ca. 550-545 Ma-old, Cadomian zircons in the UGU, and the lack of ca. 480 Ma-old, Early Ordovician zircons in the LGU hint that although the two nappe units represent relics of the same peri-Gondwanian basin, they underwent different pre-Variscan geological histories, with contrasted geotectonic settings at different times, and became juxtaposed during the Variscan orogeny.
6. Rocks from the UGU contain ca. 350-340 Ma-old metamorphic zircons providing evidence that decompression to amphibolite facies conditions, occurred during the early Carboniferous in this part of the EMC. The lack of such zircons in the LGU and, conversely, the emplacement of ca. 323 Ma-old granite dikes showing zircon inheritance from both the UGU and LGU, bracket the juxtaposition of the two units between ca. 340 and 325 Ma.
7. The UGU and the LGU were intruded by numerous granite dikes between 323 and 308 Ma (Fig. 13). These dikes indicate that the crust of the EMC remained partially molten for about 15 Ma until gravitational collapse and exhumation of the Velay granite-migmatite dome at 308 Ma.
8. The crust of the EMC derives from the reworking of sediments sourced by two main crustal components of the Gondwana supercontinent, i.e. Archean (3.3-2.7 Ga)-Paleoproterozoic (2.1-1.9 Ga) crust in one hand; and Neoproterozoic (0.8-0.6 Ga) juvenile crust on the other hand. Mixing between these crustal components took place

by magmatism during the Pan-African orogenies and/or by mechanical mixture of detritus that fed the sedimentary protoliths of the LGU and UGU paragneisses during the Ediacaran. No evidence supports the existence of an autochthonous crust older than ca. 550 Ma in the EMC.

We show that in spite of the high-grade rocks and pervasive crustal melting commonly present in the internal zone of orogens, which significantly obscures previous geological record, zircon is able to provide otherwise inaccessible insight into the polyphased magmatic, metamorphic and sedimentary history of the rocks. As demonstrated, this approach appears instrumental if we are to fully understand the role of inherited geological history in orogenic processes and the formation and the evolution of the crustal evolution in complex terrains.

Acknowledgment

We acknowledge fundings from the CNRS/INSU (Syster and PNP projects); the European Commission and the UJM through the Campus France PRESTIGE program to C.C.M.; and the Deutscher Akademischer Austauschdienst (grant A/13/70682) to O.L.. A. Gerdes, L. Marko and F.-X. d'Abzac are greatly acknowledged for their skilled technical support during Hf isotope analyses. Urs Schaltegger is thanked for permitting access to the LA-MC-ICPMS lab at the University of Geneva. We are grateful to J. Shaw, D. Avigad, C. Balica and two anonymous reviewers of which comments contributed to significantly improve the clarity of this paper.

Reference

Abati, J., Aghzer, A.M., Gerdes, A., Ennih, N., 2012. Insights on the crustal evolution of the West African Craton from Hf isotopes in detrital zircons from the Anti-Atlas belt. Precambrian Res. 212, 263–274. doi:10.1016/j.precamres.2012.06.005

Abbo, A., Avigad, D., Gerdes, A., Güngör, T., 2015. Cadomian basement and Paleozoic to Triassic siliciclastics of the Taurides (Karacahisar dome, south-central Turkey): Paleogeographic constraints from U–Pb–Hf in zircons. Lithos 227, 122–139.

doi:10.1016/j.lithos.2015.03.023
Abdelsalam, M.G., Liégeois, J.-P., Stern, R.J., 2002. The Saharan Metacraton. Journal of African Earth Sciences 34, 119–136. doi:10.1016/S0899-5362(02)00013-1
Albert, R., Arenas, R., Gerdes, A., Sánchez Martínez, S., Fernández-Suárez, J., Fuenlabrada, J.M., 2015. Provenance of the Variscan Upper Allochthon (Cabo Ortegal Complex, NW Iberian Massif). Gondwana Res. 28, 1434–1448. doi:10.1016/j.gr.2014.10.016
Alexandre, P., 2007. U–Pb zircon SIMS ages from the French Massif Central and implication for the pre-Variscan tectonic evolution in Western Europe. Comptes Rendus Geoscience 339, 613–621. doi:10.1016/j.crte.2007.07.008
Alexandrov, P., Floc'h, J.-P., Cuney, M., Cheilletz, A., 2001. Datation U–Pb à la microsonde ionique des zircons de l'unité supérieure de gneiss dans le Sud Limousin, Massif central. Comptes Rendus de l'Académie des Sciences - Series IIA - Earth and Planetary Science 332, 625–632. doi:10.1016/S1251-8050(01)01586-5
Amelin, Y., Lee, D.C., Halliday, A.N., 2000. Early-middle archaean crustal evolution deduced from Lu-Hf and U-Pb isotopic studies of single zircon grains. Geochim. Cosmochim. Ac. 64, 4205–4225. doi:10.1016/S0016-7037(00)00493-2
Avigad, D., Gerdes, A., Morag, N., Bechstadt, T., 2012. Coupled U–Pb–Hf of detrital zircons of Cambrian sandstones from Morocco and Sardinia: Implications for provenance and Precambrian crustal evolution of North Africa. Gondwana Res. 21, 690–703. doi:10.1016/j.gr.2011.06.005
Avigad, D., Weissbrod, T., Gerdes, A., Zlatkin, O., Ireland, T.R., Morag, N., 2015. The detrital zircon U–Pb–Hf fingerprint of the northern Arabian–Nubian Shield as reflected by a Late Ediacaran arkosic wedge (Zenifim Formation; subsurface Israel). Precambrian Res. 266, 1–11. doi:10.1016/j.precamres.2015.04.011
Bahlburg, H., Vervoort, J.D., DuFrane, S.A., 2010. Plate tectonic significance of Middle Cambrian and Ordovician siliciclastic rocks of the Bavarian Facies, Armorican Terrane Assemblage, Germany — U–Pb and Hf isotope evidence from detrital zircons. Gondwana Res. 17, 223–235. doi:10.1016/j.gr.2009.11.007
Balintoni, I., Balica, C., Ducea, M.N., Hann, H.-P., 2014. Peri-Gondwanan terranes in the Romanian Carpathians: A review of their spatial distribution, origin, provenance, and evolution. Geoscience Frontiers 5, 395–411. doi:10.1016/j.gsf.2013.09.002
Ballèvre, M., Le Goff, E., Hebert, R., 2001. The tectonothermal evolution of the Cadomian belt of northern Brittany, France: a Neoproterozoic volcanic arc. Tectonophysics 331, 19–43. doi:10.1016/s0040-1951(00)00234-1
Ballèvre, M., Martínez Catalán, J.R., López-Carmona, A., Pitra, P., Abati, J., Díez Fernández, R., Ducassou, C., Arenas, R., Bosse, V., Castiñeiras, P., Fernández-Suárez, J., Gómez Barreiro, J., Paquette, J.L., Peucat, J.J., Poujol, M., Ruffet, G. and Sánchez Martínez, S., 2014. Correlation of the nappe stack in the Ibero-Armorican arc across the Bay of Biscay: a joint French–Spanish project. *in* Schulmann, K., Martínez Catalán, J.R , Lardeaux, J.M., Janoušek, V. & Oggiano, G. (eds). Geological Society London, Special Publication: 405, 77–113.
Barbey, P., Marignac, C., Montel, J.M., Macaudiere, J., Gasquet, D., Jabbori, J., 1999. Cordierite Growth Textures and the Conditions of Genesis and Emplacement of Crustal Granitic Magmas: the Velay Granite Complex (Massif Central, France). J. Petrol. 40, 1425–1441. doi:10.1093/petroj/40.9.1425
Barbey, P., Villaros, A., Marignac, C., Montel, J.-M., 2015. Multiphase melting, magma emplacement and P-T-time path in late-collisional context: the Velay example (Massif Central, France). Bulletin de la Societe Geologique de France 186, 93–116. doi:10.2113/gssgfbull.186.2-3.93
Batumike, J.M., Griffin, W.L., O'Reilly, S.Y., Belousova, E.A., Pawlitschek, M., 2009.

Crustal evolution in the central Congo-Kasai Craton, Luebo, D.R. Congo: Insights from zircon U–Pb ages, Hf-isotope and trace-element data. Precambrian Res. 170, 107–115. doi:10.1016/j.precamres.2008.12.001

Be Mezeme, E., Cocherie, A., Faure, M., Legendre, O., Rossi, P., 2006. Electron microprobe monazite geochronology of magmatic events: Examples from Variscan migmatites and granitoids, Massif Central, France. Lithos 87, 276–288. doi:10.1016/j.lithos.2005.06.011

Bellot, J.P., Laverne, C., Bronner, G., 2010. An early Palaeozoic supra-subduction lithosphere in the Variscides: new evidence from the Maures massif. Int J Earth Sci (Geol Rundsch) 99, 473–504. doi:10.1007/s00531-009-0416-6

Berger, J., Féménias, O., Mercier, J.C.C., Demaiffe, D., 2006. A Variscan slow-spreading ridge (MOR-LHOT) in Limousin (French Massif Central): magmatic evolution and tectonic setting inferred from mineral chemistry. Mineral. Mag. 70, 175–185. doi:10.1180/0026461067020322

Berger, J., Féménias, O., Ohnenstetter, D., Bruguier, O., Plissart, G., Mercier, J.-C.C., Demaiffe, D., 2010. New occurrence of UHP eclogites in Limousin (French Massif Central): Age, tectonic setting and fluid-rock interactions. Lithos 118, 365–382. doi:10.1016/j.lithos.2010.05.013

Blichert-Toft, J., 2008. The Hf isotopic composition of zircon reference material 91500. Chem. Geol. 253, 252–257. doi:10.1016/j.chemgeo.2008.05.014

Block, S., Baratoux, L., Zeh, A., Laurent, O., Bruguier, O., Jessell, M., Ailleres, L., Sagna, R., Parra-Avila, L.A., Bosch, D., 2016. Paleoproterozoic juvenile crust formation and stabilisation in the south-eastern West African Craton (Ghana); New insights from U-Pb-Hf zircon data and geochemistry. Precambrian Res. 287, 1–30. doi:10.1016/j.precamres.2016.10.011

Blundy, J., Wood, B., 1994. Prediction of crystal-melt partition coefficients from elastic moduli. Nature 372, 452–454. doi:10.1038/372452a0

Bouchardon, J.-L., Santallier, D., Briand, B., Ménot, R.-P., Piboule, M., 1989. Eclogites in the French Palaeozoic Orogen: geodynamic significance. Tectonophysics 169, 317–332. doi:10.1016/0040-1951(89)90094-2

Bouilhol, P., Leyreloup, A.F., Delor, C., Vauchez, A., Monié, P., 2006. Relationships between lower and upper crust tectonic during doming: the mylonitic southern edge of the Velay metamorphic core complex (Cévennes-French Massif Central). Geodinamica Acta 19, 137–153. doi:10.3166/ga.19.137-153

Boutin, R., Montigny, R., 1993. Datation ^{40}Ar-^{39}Ar des amphibolites du complexes leptynoamphibolique du Plateau d'Aigurande : collision varisque à 390 Ma dans le Nord-Ouest du Massif Central français. Comptes rendus de l'Académie des sciences. Série 2, Mécanique, Physique, Chimie, Sciences de l'univers, Sciences de la Terre 316, 1391–1398.

Bradley, D.C., 2011. Secular trends in the geologic record and the supercontinent cycle. Earth Sci. Rev. 108, 16–33. doi:10.1016/j.earscirev.2011.05.003

Briand, B., Piboule, M., Santallier, D., Bouchardon, J.L., 1991. Geochemistry and tectonic implications of two Ordovician bimodal igneous complexes, southern French Massif Central. Journal of the Geological Society 148, 959–971. doi:10.1144/gsjgs.148.6.0959

Burg, J.P., Brun, J.P., van den Driessche, J., 1990. Le sillon houiller du Massif Central français : faille de transfert pendant l'amincissement crustal de la chaîne. Comptes rendus de l'Académie des sciences. Série 2, Mécanique, Physique, Chimie, Sciences de l'univers, Sciences de la Terre 311, 147–152.

Burg, J.-P., Vanderhaeghe, O., 1993. Structures and way-up criteria in migmatites, with application to the Velay dome (French Massif Central). Journal of Structural Geology 15, 1293–1301. doi:10.1016/0191-8141(93)90103-H

Caen-Vachette, M., 1979. Age cambrien des rhyolites transformées en leptynites dans la série mé tamorphique du Pilat (Massif Central francais). CR Acad. Sci. Paris, 289, 997–1000.

Castiñeiras, P., Navidad, M., Liesa, M., Carreras, J., Casas, J.M., 2008. U–Pb zircon ages (SHRIMP) for Cadomian and Early Ordovician magmatism in the Eastern Pyrenees: New insights into the pre-Variscan evolution of the northern Gondwana margin. Tectonophysics 461, 228–239. doi:10.1016/j.tecto.2008.04.005

Chenevoy, M., Montjuvent, G., Mandier, P., Bambier, A., Bornand, M., Combier, J., Debromez, J.-F., 1979. Carte géologique de la France à 1/50000: Feuille de Tournon. BRGM n°794.

Cocks, L.R.M., Torsvik, T.H., 2002. Earth geography from 500 to 400 million years ago: a faunal and palaeomagnetic review. Journal of the Geological Society 159, 631–644. doi:10.1144/0016-764901-118

Condie, K.C., Bickford, M.E., Aster, R.C., Belousova, E., Scholl, D.W., 2011. Episodic zircon ages, Hf isotopic composition, and the preservation rate of continental crust. Geol. Soc. Am. Bull 123, 951–957. doi:10.1130/B30344.1

Corfu, F., 2013. A century of U-Pb geochronology: The long quest towards concordance. Geol. Soc. Am. Bull 125, 33–47. doi:10.1130/B30698.1

Costa, S., Maluski, H., 1988. Datations par la méthode 39Ar-40Ar de matériel magmatique et métamorphique paléozoïque provenant du forage de Couy-Sancerre (Cher, France). Programme G.P.F. Comptes rendus de l"Académie des sciences. Série 2, Mécanique, Physique, Chimie, Sciences de l"univers, Sciences de la Terre 306, 351–356.

Costa, S., Maluski, H., Lardeaux, J.-M., 1993. ^{40}Ar-^{39}Ar chronology of Variscan tectono-metamorphic events in an exhumed crustal nappe: the Monts du Lyonnais complex (Massif Central, France). Chem. Geol. 105, 339–359. doi:10.1016/0009-2541(93)90135-6

Couzinié, S., Moyen, J.F., Villaros, A., Paquette, J.L., Scarrow, J.H., Marignac, C., 2014. Temporal relationships between Mg-K mafic magmatism and catastrophic melting of the Variscan crust in the southern part of Velay Complex (Massif Central, France). J Geosci 69–86. doi:10.3190/jgeosci.155

Couzinie, S., Laurent, O., Moyen, J.-F., Zeh, A., Bouilhol, P., Villaros, A., 2016. Post-collisional magmatism: Crustal growth not identified by zircon Hf–O isotopes. Earth Planet. Sci. Lett. 456, 182–195. doi:10.1016/j.epsl.2016.09.033

Dewey, J.F., Burke, K.C.A., 1973. Tibetan, Variscan, and Precambrian Basement Reactivation: Products of Continental Collision. J. Geol. 81, 683–692. doi:10.1086/627920

Didier, A., Bosse, V., Boulvais, P., Bouloton, J., Paquette, J.L., Montel, J.M., Devidal, J.L., 2013. Disturbance versus preservation of U–Th–Pb ages in monazite during fluid–rock interaction: textural, chemical and isotopic in situ study in microgranites (Velay Dome, France). Contrib. Mineral. Petrol. 165, 1051–1072. doi:10.1007/s00410-012-0847-0

Díez Fernández, R., Castiñeiras, P., Gómez Barreiro, J., 2012. Age constraints on Lower Paleozoic convection system: Magmatic events in the NW Iberian Gondwana margin. Gondwana Res. 21, 1066–1079. doi:10.1016/j.gr.2011.07.028

Díez Fernández, R., Martínez Catalán, J.R., Gerdes, A., Abati, J., Arenas, R., Fernández-Suárez, J., 2010. U–Pb ages of detrital zircons from the Basal allochthonous units of NW Iberia: Provenance and paleoposition on the northern margin of Gondwana during the Neoproterozoic and Paleozoic. Gondwana Res. 18, 385–399. doi:10.1016/j.gr.2009.12.006

Do Couto, D., Faure, M., Augier, R., Cocherie, A., Rossi, P., Li, X.-H., Lin, W., 2015. Monazite U–Th–Pb EPMA and zircon U–Pb SIMS chronological constraints on the tectonic, metamorphic, and thermal events in the inner part of the Variscan orogen, example from the Sioule series, French Massif Central. Int J Earth Sci (Geol Rundsch) 1–

23. doi:10.1007/s00531-015-1184-0
Downes, H., Shaw, A., Williamson, B.J., Thirlwall, M.F., 1997. Sr, Nd al36 (1997) 99–122 Hercynian granodiorites and monzogranites, Massif Central, France. Chem. Geol. 136, 99–122. doi:10.1016/S0009-2541(96)00141-6
Drost, K., Gerdes, A., Jeffries, T., Linnemann, U., Storey, C., 2011. Provenance of Neoproterozoic and early Paleozoic siliciclastic rocks of the Teplá-Barrandian unit (Bohemian Massif): Evidence from U–Pb detrital zircon ages. Gondwana Res. 19, 213–231. doi:10.1016/j.gr.2010.05.003
Ducrot, J., Lancelot, J., Marchand, J., 1983. Datation U-Pb sur zircons de l'éclogite de La Borie (Haut-Allier, France) et conséquences sur l'évolution ante-hercynienne de l'Europe occidentale. Earth Planet. Sci. Lett. 62, 385–394. doi:10.1016/0012-821X(83)90009-2
Dupraz, J., Didier, J., 1988. Le complexe anatectique du Velay (Massif central français): structure d'ensemble et évolution géologique. Géologie de la France, 4, 73-88.
Duthou, J.L., Chenevoy, M., Gay, M., 1994. Age Rb-Sr, Dévonien moyen des migmatites à cordiérite du Lyonnais (Massif central français). Comptes rendus de l'Académie des sciences. Série 2. Sciences de la terre et des planètes 319, 791–796.
Duthou, J.L., Cantagrel, J.M., Didier, J., Vialette, Y., 1984. Palaeozoic granitoids from the French Massif Central: age and origin studied by ^{87}Rb–^{87}Sr system. Physics of the Earth and Planetary Interiors 35, 131–144. doi:10.1016/0031-9201(84)90039-6
Eglinger, A., Thébaud, N., Zeh, A., Davis, J., Miller, J., Parra-Avila, L.A., Loucks, R., McCuaig, C., 2016. New insights into the crustal growth of the Paleoproterozoic margin of the Archean Kéména-Man domain, West African craton (Guinea): Implications for gold mineral system. Precambrian Res. doi:10.1016/j.precamres.2016.11.012
Faure, M., 1995. Late orogenic carboniferous extensions in the Variscan French Massif Central. Tectonics 14, 132–153. doi:10.1029/94TC02021
Faure, M., Cocherie, A., Mézème, E.B., Charles, N., Rossi, P., 2010. Middle Carboniferous crustal melting in the Variscan Belt: New insights from U–Th–Pb_{tot}. monazite and U–Pb zircon ages of the Montagne Noire Axial Zone (southern French Massif Central). Gondwana Res. 18, 653–673. doi:10.1016/j.gr.2010.02.005
Faure, M., Lardeaux, J.-M., Ledru, P., 2009. A review of the pre-Permian geology of the Variscan French Massif Central. Comptes Rendus Geoscience 341, 202–213. doi:10.1016/j.crte.2008.12.001
Faure, M., Charonnat, X., Chauvet, A., Chen, Y., Talbot, J.-Y., Martelet, G., Courrioux, G., Monié, P., Milesi, J.-P., 2001. Tectonic evolution of the Cevennes para-autochthonous domain of the Hercynian French Massif Central and its bearing on ore deposits formation. Bulletin de la Societe Geologique de France 172, 687–696. doi:10.2113/172.6.687
Fernández-Suárez, J., Gutiérrez-Alonso, G., 2000. New ideas on the Proterozoic-Early Palaeozoic evolution of NW Iberia: insights from U–Pb detrital zircon ages. Precambrian Res. 102, 185–206. doi:10.1016/s0301-9268(00)00065-6
Feybesse, J.L., Lardeaux, J.M., Johan, V., Tegyey, M., Dufour, E., Lemiere, B., Delfour, J., 1988. La série de la Brévenne (Massif central français): une unité dévonienne charriée sur le complexe métamorphique des Monts du Lyonnais à la fin de la collision varisque. Comptes rendus de l"Académie des sciences. Série 2, Mécanique, Physique, Chimie, Sciences de l"univers, Sciences de la Terre 307, 991–996.
Fortey, R.A., Cocks, L.R.M., 2003. Palaeontological evidence bearing on global Ordovician–Silurian continental reconstructions. Earth Sci. Rev. 61, 245–307. doi:10.1016/S0012-8252(02)00115-0
Franke, W., 2014. Topography of the Variscan orogen in Europe: failed–not collapsed. Int J Earth Sci (Geol Rundsch) 103, 1471–1499. doi:10.1007/s00531-014-1014-9
Gardien, V., 1993. Les reliques pétrologiques de haute à moyenne pression des séries du

Vivarais oriental (Est du Massif Central français). Comptes rendus de l"Académie des sciences. Série 2, Mécanique, Physique, Chimie, Sciences de l"univers, Sciences de la Terre 316, 1247–1254.

Gardien, V., Tegyey, M., Lardeaux, J.M., Missery, M., Dufour, E., 1990. Crust-mantle relationships in the French Variscan chain: the example of the Southern Monts du Lyonnais unit (eastern French Massif Central). J Metamorph Geol 8, 477–492. doi:10.1111/j.1525-1314.1990.tb00481.x

Gardien, V., Lardeaux, J.-M., Ledru, P., Allemand, P., Guillot, S., 1997. Metamorphism during late orogenic extension; insights from the French Variscan belt. Bulletin de la Societe Geologique de France 168, 271–286.

Garfunkel, Z., 2015. The relations between Gondwana and the adjacent peripheral Cadomian domain—constrains on the origin, history, and paleogeography of the peripheral domain. Gondwana Res. 28, 1257–1281. doi:10.1016/j.gr.2015.05.011

Gebauer, D., Williams, I.S., Compston, W., Grünenfelder, M., 1989. The development of the Central European continental crust since the Early Archaean based on conventional and ion-microprobe dating of up to 3.84 b.y. old detrital zircons. Tectonophysics 157, 81–96.

Gerdes, A., Zeh, A., 2006. Combined U Pb and Hf isotope LA-(MC-)ICP-MS analyses of detrital zircons: Comparison with SHRIMP and new constraints for the provenance and age of an Armorican metasediment in Central Germany. Earth Planet. Sci. Lett. 249, 47–61. doi:10.1016/j.epsl.2006.06.039

Gerdes, A., Zeh, A., 2009. Zircon formation versus zircon alteration — New insights from combined U–Pb and Lu–Hf in-situ LA-ICP-MS analyses, and consequences for the interpretation of Archean zircon from the Central Zone of the Limpopo Belt. Chem. Geol. 261, 230–243. doi:10.1016/j.chemgeo.2008.03.005

Griffin, W.L., Wang, X., Jackson, S.E., Pearson, N.J., O'Reilly, S.Y., Xu, X., Zhou, X., 2002. Zircon chemistry and magma mixing, SE China: In-situ analysis of Hf isotopes, Tonglu and Pingtan igneous complexes. Lithos 61, 237–269.

Harley, S.L., Kelly, N.M., 2007. Zircon Tiny but Timely. Elements 3, 13–18. doi:10.2113/gselements.3.1.13

Henderson, B.J., Collins, W.J., Murphy, J.B., Gutiérrez-Alonso, G., Hand, M., 2015. Gondwanan basement terranes of the Variscan–Appalachian orogen: Baltican, Saharan and West African hafnium isotopic fingerprints in Avalonia, Iberia and the Armorican Terranes. Tectonophysics. doi:10.1016/j.tecto.2015.11.020

Hoskin, P.W.O., Schaltegger, U., 2003. The composition of zircon and igneous and metamorphic petrogenesis. Rev. Mineral. Geochem. 53, 27–62. doi:10.2113/0530027

Innocent, C., Michard, A., Guerrot, C., Hamelin, B., 2003. U-Pb zircon age of 548 Ma for the leptynites (high-grade felsic rocks) of the central part of the Maures Massif. Geodynamic significance of the so-called leptyno-amphibolitic complexes of the Variscan belt of western Europe. Bulletin de la Societe Geologique de France 174, 585–594. doi:10.2113/174.6.585

Jackson, S.E., Pearson, N.J., Griffin, W.L., Belousova, E.A., 2004. The application of laser ablation-inductively coupled plasma-mass spectrometry to in situ U–Pb zircon geochronology. Chem. Geol. 211, 47–69. doi:10.1016/j.chemgeo.2004.06.017

Keay, S., Lister, G., 2002. African provenance for the metasediments and metaigneous rocks of the Cyclades, Aegean Sea, Greece. Geology 30, 235–238. doi:10.1130/0091-7613(2002)030<0235:APFTMA>2.0.CO;2

Kemp, A.I.S., Foster, G.L., Schersten, A., Whitehouse, M.J., Darling, J., Storey, C., 2009. Concurrent Pb–Hf isotope analysis of zircon by laser ablation multi-collector ICP-MS, with implications for the crustal evolution of Greenland and the Himalayas. Chem. Geol. 261, 244–260. doi:10.1016/j.chemgeo.2008.06.019

Kemp, A.I.S., Hawkesworth, C.J., Paterson, B.A., Kinny, P.D., 2006. Episodic growth of the Gondwana supercontinent from hafnium and oxygen isotopes in zircon. Nature 439, 580–583. doi:10.1038/nature04505

Keppie, J.D., Nance, R.D., Murphy, J.B., Dostal, J., 2003. Tethyan, Mediterranean, and Pacific analogues for the Neoproterozoic–Paleozoic birth and development of peri-Gondwanan terranes and their transfer to Laurentia and Laurussia. Tectonophysics 365, 195–219. doi:10.1016/S0040-1951(03)00037-4

Kolodner, K., Avigad, D., McWilliams, M., Wooden, J.L., Weissbrod, T., Feinstein, S., 2006. Provenance of north Gondwana Cambrian–Ordovician sandstone: U–Pb SHRIMP dating of detrital zircons from Israel and Jordan. Geological Magazine 143, 367. doi:10.1017/S0016756805001640

Kroner, U., Romer, R.L., 2013. Two plates — Many subduction zones: The Variscan orogeny reconsidered. Gondwana Res. 24, 298–329. doi:10.1016/j.gr.2013.03.001

Lafon, J. M., 1984. La granodiorite de Caplongue, nouveau témoin d'un magmatisme cambrien dans le Rouergue oriental. Comptes-rendus des séances de l'Académie des sciences. Série 2, Mécanique-physique, chimie, sciences de l'univers, sciences de la terre, 298(14), 595–600.

Lardeaux, J.M., Ledru, P., Daniel, I., Duchene, S., 2001. The Variscan French Massif Central—a new addition to the ultra-high pressure metamorphic "club": exhumation processes and geodynamic consequences. Tectonophysics 332, 143–167. doi:10.1016/S0040-1951(00)00253-5

Lardeaux, J.M., Schulmann, K., Faure, M., Janoucek, V., Lexa, O., Skrzypek, E., Edel, J.B., tipska, P., 2014. The Moldanubian Zone in the French Massif Central, Vosges/Schwarzwald and Bohemian Massif revisited: differences and similarities. Geol. Soc. London, Special Publications 405, 7–44. doi:10.1144/SP405.14

Laurent, O., Couzinie, S., Zeh, A., Vanderhaeghe, O., Moyen, J.-F., Villaros, A., Gardien, V., Chelle-Michou, C., 2017. Protracted, coeval crust and mantle melting during Variscan late-orogenic evolution: U–Pb dating in the eastern French Massif Central. Int J Earth Sci (Geol Rundsch) 1–31. doi:10.1007/s00531-016-1434-9

Ledru, P., Courrioux, G., Dallain, C., Lardeaux, J.M., Montel, J.M., Vanderhaeghe, O., Vitel, G., 2001. The Velay dome (French Massif Central): melt generation and granite emplacement during orogenic evolution. Tectonophysics 342, 207–237. doi:10.1016/S0040-1951(01)00165-2

Ledru, P., Lardeaux, J.M., Santallier, D., Autran, A., Quenardel, J.M., Floc'h, J.P., Lerouge, G., Maillet, N., Marchand, J., Ploquin, A., 1989. Ou sont les nappes dans le massif central francais? Bulletin de la Societe Geologique de France V, 605–618. doi:10.2113/gssgfbull.V.3.605

Lenting, C., Geisler, T., Gerdes, A., Kooijman, E., Scherer, E.E., Zeh, A., 2010. The behavior of the Hf isotope system in radiation-damaged zircon during experimental hydrothermal alteration. Am. Mineral. 95, 1343–1348. doi:10.2138/am.2010.3521

Lévêque, M.-H., 1985. Mise en évidence d'un témoin d'un socle précambrien dans le Massif Central français: l'orthogneiss des Palanges (Aveyron). Comptes-rendus des séances de l'Académie des sciences. Série 2, Mécanique-physique, chimie, sciences de l'univers, sciences de la terre. 300, 277-282.

Linnemann, U., Gerdes, A., Hofmann, M., Marko, L., 2014. The Cadomian Orogen: Neoproterozoic to Early Cambrian crustal growth and orogenic zoning along the periphery of the West African Craton—Constraints from U–Pb zircon ages and Hf isotopes (Schwarzburg Antiform, Germany). Precambrian Res. 244, 236–278. doi:10.1016/j.precamres.2013.08.007

Linnemann, U., McNaughton, N.J., Romer, R.L., Gehmlich, M., Drost, K., Tonk, C., 2004.

West African provenance for Saxo-Thuringia (Bohemian Massif): Did Armorica ever leave pre-Pangean Gondwana? ? U/Pb-SHRIMP zircon evidence and the Nd-isotopic record. Int J Earth Sci (Geol Rundsch) 93, 683–705. doi:10.1007/s00531-004-0413-8

Linnemann, U., Ouzegane, K., Drareni, A., Hofmann, M., Becker, S., Gärtner, A., Sagawe, A., 2011. Sands of West Gondwana: An archive of secular magmatism and plate interactions — A case study from the Cambro-Ordovician section of the Tassili Ouan Ahaggar (Algerian Sahara) using U-Pb-LA-ICP-MS detrital zircon ages. Lithos 123, 188–203. doi:10.1016/j.lithos.2011.01.010

Linnemann, U., Pereira, F., Jeffries, T.E., Drost, K., Gerdes, A., 2008. The Cadomian Orogeny and the opening of the Rheic Ocean: The diacrony of geotectonic processes constrained by LA-ICP-MS U–Pb zircon dating (Ossa-Morena and Saxo-Thuringian Zones, Iberian and Bohemian Massifs). Tectonophysics 461, 21–43. doi:10.1016/j.tecto.2008.05.002

Malavieille, J., 1993. Late Orogenic extension in mountain belts: Insights from the basin and range and the Late Paleozoic Variscan Belt. Tectonics 12, 1115–1130. doi:10.1029/93TC01129

Malavieille, J., Guihot, P., Costa, S., Lardeaux, J.M., Gardien, V., 1990. Collapse of the thickened Variscan crust in the French Massif Central: Mont Pilat extensional shear zone and St. Etienne Late Carboniferous basin. Tectonophysics 177, 139–149. doi:10.1016/0040-1951(90)90278-G

Matte, P., 1991. Accretionary history and crustal evolution of the Variscan belt in Western Europe. Tectonophysics 196, 309–337. doi:10.1016/0040-1951(91)90328-P

Matte, P., 2001. The Variscan collage and orogeny (480-290 Ma) and the tectonic definition of the Armorica microplate: a review. Terra Nova 13, 122–128. doi:10.1046/j.1365-3121.2001.00327.x

Meinhold, G., Morton, A.C., Avigad, D., 2013. New insights into peri-Gondwana paleogeography and the Gondwana super-fan system from detrital zircon U–Pb ages. Gondwana Res. 23, 661–665. doi:10.1016/j.gr.2012.05.003

Meinhold, G., Morton, A.C., Fanning, C.M., Frei, D., Howard, J.P., Phillips, R.J., Strogen, D., Whitham, A.G., 2011. Evidence from detrital zircons for recycling of Mesoproterozoic and Neoproterozoic crust recorded in Paleozoic and Mesozoic sandstones of southern Libya. Earth Planet. Sci. Lett. 312, 164–175. doi:10.1016/j.epsl.2011.09.056

Melleton, J., Cocherie, A., Faure, M., Rossi, P., 2010. Precambrian protoliths and Early Paleozoic magmatism in the French Massif Central: U–Pb data and the North Gondwana connection in the west European Variscan belt. Gondwana Res. 17, 13–25. doi:10.1016/j.gr.2009.05.007

Ménard, G., Molnar, P., 1988. Collapse of a Hercynian Tibetan Plateau into a late Palaeozoic European Basin and Range province. Nature 334, 235–237. doi:10.1038/334235a0

Mintrone M (2015) Le Massif Central avant la chaîne Varisque: caractérisation des orthogneiss du début du Primaire. Travail d'Étude et de Recherche, University of Clermont-Ferrand, France, p 31

Montel, J.M., Marignac, C., Barbey, P., Pichavant, M., 1992. Thermobarometry and granite genesis: the Hercynian low-P, high-T Velay anatectic dome (French Massif Central). J Metamorph Geol 10, 1–15. doi:10.1111/j.1525-1314.1992.tb00068.x

Montes, A.D., Catalán, J.R.M., Mulas, F.B., 2010. Role of the Ollo de Sapo massive felsic volcanism of NW Iberia in the Early Ordovician dynamics of northern Gondwana. Gondwana Res. 17, 363–376. doi:10.1016/j.gr.2009.09.001

Morag, N., Avigad, D., Gerdes, A., Belousova, E., Harlavan, Y., 2011a. Detrital zircon Hf isotopic composition indicates long-distance transport of North Gondwana Cambrian-

Ordovician sandstones. Geology 39, 955–958. doi:10.1130/G32184.1
Morag, N., Avigad, D., Gerdes, A., Belousova, E., Harlavan, Y., 2011b. Crustal evolution and recycling in the northern Arabian-Nubian Shield: New perspectives from zircon Lu–Hf and U–Pb systematics. Precambrian Res. 186, 101–116. doi:10.1016/j.precamres.2011.01.004
Morag, N., Avigad, D., Gerdes, A., Harlavan, Y., 2012. 1000–580 Ma crustal evolution in the northern Arabian-Nubian Shield revealed by U–Pb–Hf of detrital zircons from late Neoproterozoic sediments (Elat area, Israel). Precambrian Res. 208-211, 197–212. doi:10.1016/j.precamres.2012.04.009
Morel, M.L.A., Nebel, O., Nebel-Jacobsen, Y.J., Miller, J.S., Vroon, P.Z., 2008. Hafnium isotope characterization of the GJ-1 zircon reference material by solution and laser-ablation MC-ICPMS. Chem. Geol. 255, 231–235. doi:10.1016/j.chemgeo.2008.06.040
Mougeot, R., Respaut, J.P., Ledru, P., Marignac, C., 1997. U-Pb chronology on accessory minerals of the Velay anatectic dome (French Massif Central). Eur. J. Mineral. 9, 141–156. doi:10.1127/ejm/9/1/0141
Moyen, J.F., Laurent, O., Chelle-Michou, C., Couzinié, S., Vanderhaeghe, O., Zeh, A., Villaros, A., Gardien, V., 2016. Collision vs. subduction-related magmatism: two contrasting ways of granite formation and implications for crustal growth. Lithos. doi:10.1016/j.lithos.2016.09.018
Murphy, J.B., Gutiérrez-Alonso, G., Nance, R.D., Fernández-Suárez, J., Keppie, J.D., Quesada, C., Strachan, R.A., Dostal, J., 2006. Origin of the Rheic Ocean: Rifting along a Neoproterozoic suture? Geology 34, 325. doi:10.1130/G22068.1
Næraa, T., Schersten, A., Rosing, M.T., Kemp, A.I.S., Hoffmann, J.E., Kokfelt, T.F., Whitehouse, M.J., 2012. Hafnium isotope evidence for a transition in the dynamics of continental growth 3.2 Gyr ago. Nature 485, 627–630. doi:10.1038/nature11140
Nance, R.D., Gutiérrez-Alonso, G., Keppie, J.D., Linnemann, U., Murphy, J.B., Quesada, C., Strachan, R.A., Woodcock, N.H., 2010. Evolution of the Rheic Ocean. Gondwana Res. 17, 194–222. doi:10.1016/j.gr.2009.08.001
Nance, R.D., Murphy, J.B., 1994. Contrasting basement isotopic signatures and the palinspastic restoration of peripheral orogens: Example from the Neoproterozoic Avalonian-Cadomian belt. Geology 22, 617–620. doi:10.1130/0091-7613(1994)022<0617:CBISAT>2.3.CO;2
Orejana, D., Merino Martínez, E., Villaseca, C., Andersen, T., 2015. Ediacaran–Cambrian paleogeography and geodynamic setting of the Central Iberian Zone: Constraints from coupled U–Pb–Hf isotopes of detrital zircons. Precambrian Res. 261, 234–251. doi:10.1016/j.precamres.2015.02.009
Paquette, J.-L., Piro, J.-L., Devidal, J.-L., Bosse, V., Didier, A., Sannac, S., Abdelnour, Y., 2014. Sensitivity Enhancement in LA-ICP-MS by N2 Addition to Carrier Gas: Application to Radiometric Dating of U-Th-Bearing Minerals. Agilent ICP-MS Journal 58, 4–5.
Paquette, J.L., Monchoux, P., Couturier, M., 1995. Geochemical and isotopic study of a norite-eclogite transition in the European Variscan belt: Implications for U–Pb zircon systematics in metabasic rocks. Geochim. Cosmochim. Ac. 59, 1611–1622. doi:10.1016/0016-7037(95)00067-a
Paris, F., Robardet, M., 1990. Early Palaeozoic palaeobiogeography of the Variscan regions. Tectonophysics 177, 193–213. doi:10.1016/0040-1951(90)90281-C
Parra-Avila, L.A., Belousova, E., Fiorentini, M.L., Baratoux, L., Davis, J., Miller, J., McCuaig, T.C., 2016. Crustal evolution of the Paleoproterozoic Birimian terranes of the Baoulé-Mossi domain, southern West African Craton: U–Pb and Hf-isotope studies of detrital zircons. Precambrian Res. 274, 25–60. doi:10.1016/j.precamres.2015.09.005

Pastor-Galán, D., Gutiérrez-Alonso, G., Murphy, J.B., Fernández-Suárez, J., Hofmann, M., Linnemann, U., 2013. Provenance analysis of the Paleozoic sequences of the northern Gondwana margin in NW Iberia: Passive margin to Variscan collision and orocline development. Gondwana Res. 23, 1089–1103. doi:10.1016/j.gr.2012.06.015

Pereira, M.F., Linnemann, U., Hofmann, M., Chichorro, M., Solá, A.R., Medina, J., Silva, J.B., 2012a. The provenance of Late Ediacaran and Early Ordovician siliciclastic rocks in the Southwest Central Iberian Zone: Constraints from detrital zircon data on northern Gondwana margin evolution during the late Neoproterozoic. Precambrian Res. 192-195, 166–189. doi:10.1016/j.precamres.2011.10.019

Pereira, M.F., Solá, A.R., Chichorro, M., Lopes, L., Gerdes, A., Silva, J.B., 2012b. North-Gondwana assembly, break-up and paleogeography: U–Pb isotope evidence from detrital and igneous zircons of Ediacaran and Cambrian rocks of SW Iberia. Gondwana Res. 22, 866–881. doi:10.1016/j.gr.2012.02.010

Pin, C., 1990. Variscan oceans: Ages, origins and geodynamic implications inferred from geochemical and radiometric data. Tectonophysics 177, 215–227. doi:10.1016/0040-1951(90)90282-D

Pin, C., Duthou, J.-L., 1990. Sources of Hercynian granitoids from the French Massif Central: Inferences from Nd isotopes and consequences for crustal evolution. Chem. Geol. 83, 281–296. doi:10.1016/0009-2541(90)90285-F

Pin, C., Lancelot, J., 1982. U-Pb dating of an early paleozoic bimodal magmatism in the french Massif Central and of its further metamorphic evolution. Contrib. Mineral. Petrol. 79, 1–12. doi:10.1007/BF00376956

Pin, C., Marini, F., 1993. Early Ordovician continental break-up in Variscan Europe: Nd-Sr isotope and trace element evidence from bimodal igneous associations of the Southern Massif Central, France. Lithos 29, 177–196. doi:10.1016/0024-4937(93)90016-6

Pin, C., Paquette, J.-L., 1997. A mantle-derived bimodal suite in the Hercynian Belt: Nd isotope and trace element evidence for a subduction-related rift origin of the Late Devonian Brévenne metavolcanics, Massif Central (France). Contrib. Mineral. Petrol. 129, 222–238. doi:10.1007/s004100050334

Potrel, A., Peucat, J.J., Fanning, C.M., 1998. Archean crustal evolution of the west African craton: Example of the Amsaga area (Reguibat rise). U-Pb and Sm-Nd evidence for crustal growth and recycling. Precambrian Res. 90, 107–117.

Potrel, A., Peucat, J.J., Fanning, C.M., Auvray, B., Burg, J.P., Caruba, C., 1996. 3.5 Ga old terranes in the West African Craton, Mauritania. Journal of the Geological Society 153, 507–510. doi:10.1144/gsjgs.153.4.0507

R'Kha Chaham, K., Couturié, J.P., Duthou, J.L., Fernandez, A., Vitel, G., 1990. L'orthogneiss œillé de l'Arc de Fix: un nouveau témoin d‘âge cambrien d’’un magmatisme hyper alumineux dans le Massif Central français. Comptes rendus de l'Académie des sciences. Série 2, Mécanique, Physique, Chimie, Sciences de l'univers, Sciences de la Terre 311, 845–850.

Rino, S., Kon, Y., Sato, W., Maruyama, S., Santosh, M., Zhao, D., 2008. The Grenvillian and Pan-African orogens: World's largest orogenies through geologic time, and their implications on the origin of superplume. Gondwana Res. 14, 51–72. doi:10.1016/j.gr.2008.01.001

Robardet, M., Paris, F., Racheboeuf, P.R., 1990. Palaeogeographic evolution of southwestern Europe during Early Palaeozoic times. Geological Society, London, Memoirs 12, 411–419. doi:10.1144/GSL.MEM.1990.012.01.38

Samson, S.D., D'Lemos, R.S., Blichert-Toft, J., Vervoort, J., 2003. U–Pb geochronology and Hf–Nd isotope compositions of the oldest Neoproterozoic crust within the Cadomian orogen: new evidence for a unique juvenile terrane. Earth Planet. Sci. Lett. 208, 165–180.

doi:10.1016/S0012-821X(03)00045-1
Samson, S.D., D'Lemos, R.S., Miller, B.V., Hamilton, M.A., 2005. Neoproterozoic palaeogeography of the Cadomia and Avalon terranes: constraints from detrital zircon U-Pb ages. Journal of the Geological Society 162, 65–71. doi:10.1144/0016-764904-003
Santallier, D., Briand, B., Menot, R.P., Piboule, M., 1988. Les complexes leptyno-amphiboliques (C.I.A.); revue critique et suggestions pour un meilleur emploi de ce terme. Bulletin de la Societe Geologique de France IV, 3–12. doi:10.2113/gssgfbull.IV.1.3
Shaw, J., Johnston, S.T., 2016. Terrane wrecks (coupled oroclines) and paleomagnetic inclination anomalies. Earth Sci. Rev. 154, 191–209. doi:10.1016/j.earscirev.2016.01.003
Shaw, J., Gutiérrez-Alonso, G., Johnston, S.T., Galán, D.P., 2014. Provenance variability along the Early Ordovician north Gondwana margin: Paleogeographic and tectonic implications of U-Pb detrital zircon ages from the Armorican Quartzite of the Iberian Variscan belt. Geol. Soc. Am. Bull 126, 702–719. doi:10.1130/B30935.1
Sider, H., Ohnenstetter, M., 1986. Field and petrological evidence for the development of an ensialic marginal basin related to the Hercynian orogeny in the Massif Central, France. Geol Rundsch 75, 421–443. doi:10.1007/BF01820621
Simancas, J.F., Tahiri, A., Azor, A., Lodeiro, F.G., Martínez Poyatos, D.J., Hadi, El, H., 2005. The tectonic frame of the Variscan–Alleghanian orogen in Southern Europe and Northern Africa. Tectonophysics 398, 181–198. doi:10.1016/j.tecto.2005.02.006
Sirevaag, H., Jacobs, J., Ksienzyk, A.K., Rocchi, S., Paoli, G., Jørgensen, H., Kosler, J., 2016. From Gondwana to Europe: The journey of Elba Island (Italy) as recorded by U–Pb detrital zircon ages of Paleozoic metasedimentary rocks. Gondwana Res. doi:10.1016/j.gr.2015.12.006
Skrzypek, E., Schulmann, K., Tabaud, A.S., Edel, J.B., 2014. Palaeozoic evolution of the Variscan Vosges Mountains. Geol. Soc. London, Special Publications 405, 45–75. doi:10.1144/SP405.8
Sláma, J., Košler, J., Condon, D.J., Crowley, J.L., Gerdes, A., Hanchar, J.M., Horstwood, M.S.A., Morris, G.A., Nasdala, L., Norberg, N., Schaltegger, U., Schoene, B., Tubrett, M.N., Whitehouse, M.J., 2008. Plešovice zircon — A new natural reference material for U–Pb and Hf isotopic microanalysis. Chem. Geol. 249, 1–35. doi:10.1016/j.chemgeo.2007.11.005
Solgadi, F., Moyen, J.-F., Vanderhaeghe, O., Sawyer, E.W., Reisberg, L., 2007. The role of crustal anatexis and mantle-derived magmas in the genesis of synorogenic Hercynian granites of the Livradois area, French Massif Central. The Canadian Mineralogist 45, 581–606. doi:10.2113/gscanmin.45.3.581
Squire, R.J., Campbell, I.H., Allen, C.M., Wilson, C.J.L., 2006. Did the Transgondwanan Supermountain trigger the explosive radiation of animals on Earth? Earth Planet. Sci. Lett. 250, 116–133. doi:10.1016/j.epsl.2006.07.032
Stampfli, G.M., Hochard, C., Vérard, C., Wilhem, C., von Raumer, J.F., 2013. The formation of Pangea. Tectonophysics 593, 1–19. doi:10.1016/j.tecto.2013.02.037
Tait, J., Schätz, M., Bachtadse, V., Soffel, H., 2000. Palaeomagnetism and Palaeozoic palaeogeography of Gondwana and European terranes. Geol. Soc. London, Special Publications 179, 21–34. doi:10.1144/GSL.SP.2000.179.01.04
Tait, J.A., Bachtadse, V., Franke, W., Soffel, H.C., 1997. Geodynamic evolution of the European Variscan fold belt: palaeomagnetic and geological constraints. Geol Rundsch 86, 585. doi:10.1007/s005310050165
Tchameni, R., Mezger, K., Nsifa, N.E., Pouclet, A., 2001. Crustal origin of Early Proterozoic syenites in the Congo Craton (Ntem Complex), South Cameroon. Lithos 57, 23–42. doi:10.1016/S0024-4937(00)00072-4

Teixeira, R.J.S., Neiva, A.M.R., Silva, P.B., Gomes, M.E.P., Andersen, T., Ramos, J.M.F., 2011. Combined U–Pb geochronology and Lu–Hf isotope systematics by LAM–ICPMS of zircons from granites and metasedimentary rocks of Carrazeda de Ansiães and Sabugal areas, Portugal, to constrain granite sources. Lithos 125, 321–334. doi:10.1016/j.lithos.2011.02.015

Turpin, L., Cuney, M., Friedrich, M., Bouchez, J.-L., Aubertin, M., 1990. Meta-igneous origin of Hercynian peraluminous granites in N.W. French Massif Central: implications for crustal history reconstructions. Contrib. Mineral. Petrol. 104, 163–172. doi:10.1007/BF00306440

Vanderhaeghe, O., 2009. Migmatites, granites and orogeny: Flow modes of partially-molten rocks and magmas associated with melt/solid segregation in orogenic belts. Tectonophysics 477, 119–134. doi:10.1016/j.tecto.2009.06.021

Vanderhaeghe, O., Burg, J.-P., Teyssier, C., 1999. Exhumation of migmatites in two collapsed orogens: Canadian Cordillera and French Variscides. Geol. Soc. London, Special Publications 154, 181–204. doi:10.1144/GSL.SP.1999.154.01.08

Vanderhaeghe, O., Teyssier, C., 2001. Crustal-scale rheological transitions during late-orogenic collapse. Tectonophysics 335, 211–228. doi:10.1016/S0040-1951(01)00053-1

Veevers, J.J., 2004. Gondwanaland from 650–500 Ma assembly through 320 Ma merger in Pangea to 185–100 Ma breakup: supercontinental tectonics via stratigraphy and radiometric dating. Earth Sci. Rev. 68, 1–132. doi:10.1016/j.earscirev.2004.05.002

Vermeesch, P., 2013. Multi-sample comparison of detrital age distributions. Chem. Geol. 341, 140–146. doi:10.1016/j.chemgeo.2013.01.010

Villaseca, C., Castineiras, P., Orejana, D., 2015. Early Ordovician metabasites from the Spanish Central System: A remnant of intraplate HP rocks in the Central Iberian Zone. Gondwana Res. 27, 392–409. doi:10.1016/j.gr.2013.10.007

Villaseca, C., Merino Martínez, E., Orejana, D., Andersen, T., Belousova, E., 2016. Zircon Hf signatures from granitic orthogneisses of the Spanish Central System: Significance and sources of the Cambro-Ordovician magmatism in the Iberian Variscan Belt. Gondwana Res. 34, 60–83. doi:10.1016/j.gr.2016.03.004

von Raumer, J.F., Bussy, F., Schaltegger, U., Schulz, B., Stampfli, G.M., 2013. Pre-Mesozoic Alpine basements—Their place in the European Paleozoic framework. Geol. Soc. Am. Bull 125, 89–108. doi:10.1130/B30654.1

von Raumer, J.F., Stampfli, G.M., 2008. The birth of the Rheic Ocean — Early Palaeozoic subsidence patterns and subsequent tectonic plate scenarios. Tectonophysics 461, 9–20. doi:10.1016/j.tecto.2008.04.012

von Raumer, J.F., Stampfli, G.M., Arenas, R., Sánchez Martínez, S., 2015. Ediacaran to Cambrian oceanic rocks of the Gondwana margin and their tectonic interpretation. Int J Earth Sci (Geol Rundsch) 104, 1–15. doi:10.1007/s00531-015-1142-x

von Raumer, J.F., Stampfli, G.M., Bussy, F., 2003. Gondwana-derived microcontinents — the constituents of the Variscan and Alpine collisional orogens. Tectonophysics 365, 7–22. doi:10.1016/S0040-1951(03)00015-5

Weisbrod, A., Pichavant, M., Marignac, C., Macaudière, J., Leroy, J., 1980. Relations structurales et chronologiques entre le magmatisme basique, les granitisations et l'évolution tectonométamorphique tardi-hercynienne dans les Cévennes médianes, Massif central Français. CR Acad. Sci., Paris. 291, 665-668.

Wiedenbeck, M., Allé, P., Corfu, F., Griffin, W.L., Meier, M., Oberli, F., Quadt, von, A., Roddick, J.C., Spiegel, W., 1995. Three natural zircon standards for U-Th-Pb, Lu-Hf, trace element and REE analyses. Geostandards and Geoanalytical Res. 19, 1–23. doi:10.1111/j.1751-908X.1995.tb00147.x

Williams, I.S., Fiannacca, P., Cirrincione, R., Pezzino, A., 2012. Peri-Gondwanan origin and

early geodynamic history of NE Sicily: A zircon tale from the basement of the Peloritani Mountains. Gondwana Res. 22, 855–865. doi:10.1016/j.gr.2011.12.007

Williamson, B.J., Downes, H., Thirlwall, M.F., Beard, A., 1997. Geochemical constraints on restite composition and unmixing in the Velay anatectic granite, French Massif Central. Lithos 40, 295–319. doi:10.1016/S0024-4937(97)00033-9

Williamson, B.J., Shaw, A., Downes, H., Thirlwall, M.F., 1996. Geochemical constraints on the genesis of Hercynian two-mica leucogranites from the Massif Central, France. Chem. Geol. 127, 25–42. doi:10.1016/0009-2541(95)00105-0

Woodhead, J.D., Hergt, J.M., 2005. A Preliminary Appraisal of Seven Natural Zircon Reference Materials for In Situ Hf Isotope Determination. Geostandards and Geoanalytical Res. 29, 183–195. doi:10.1111/j.1751-908X.2005.tb00891.x

Zeh, A., Brätz, H., Millar, I.L., Williams, I.S., 2001. A combined zircon SHRIMP and Sm–Nd isotope study of high-grade paragneisses from the Mid-German Crystalline Rise: evidence for northern Gondwanan and Grenvillian provenance. Journal of the Geological Society 158, 983–994. doi:10.1144/0016-764900-186

Zeh, A., Gerdes, A., Will, T. M. & Frimmel, H. (2010a). Hafnium isotope homogenization during metamorphic zircon growth in amphibolite-facies rocks, examples from the Shackleton Range (Antarctica). Geochim. Cosmochim. Acta, 74, 4740-4758

Zeh, A., Gerdes. A., Barton, J. M. Jr., Klemd, R., (2010b). U-Th-Pb and Lu-Hf systematics of zircon from TTG's, leucosomes, anorthosites and quartzites of the Limpopo Belt (South Africa): constraints for the formation, recycling, and metamorphism of Paleoarchean crust. Precambrian Res., 179, 50-68. doi:10.1016/j.precamres.2010.02.012

Zeh, A., Gerdes, A., 2010. Baltica- and Gondwana-derived sediments in the Mid-German Crystalline Rise (Central Europe): Implications for the closure of the Rheic ocean. Gondwana Res. 17, 254–263. doi:10.1016/j.gr.2009.08.004

Figures

Fig. 1. Geological map and generalized cross-section of the eastern Massif Central and location of the studied area (adapted from Moyen et al., 2016). Inset shows the distribution of the Variscan terranes throughout Europe (adapted from Ballèvre et al., 2014). Am: amphibole; bio: biotite; crd: cordierite ms: muscovite;

Fig. 2. Geological map and cross-section of the Tournon area and sample location (modified from Chenevoy et al., 1979). Bio: biotite; crd: cordierite; ms: muscovite; sill: sillimanite;

Fig. 3. Representative zircon CL-images for each dated sample. The $^{206}Pb/^{238}U$ dates are reported next to their respective spots. Dates in italics indicate discordant data (< 98% concordance)

Fig. 4. LA-ICPMS zircon U-Pb dating results from the Upper Gneiss Unit (UGU). Left column presents the Tera-Wasserburg diagrams. Ellipses in red were used to calculate the Concordia (yellow ellipses) or intercept ages. Right column presents the ranked $^{206}Pb/^{238}U$ dates of concordant analyses and the corresponding density plots. Dates in black were used to calculate the weighted mean ages (dark grey vertical box). Circles below the x-axis are the central value of individual data points. All uncertainties are given at 95% confidence (2σ).

Fig. 5. LA-ICPMS zircon U-Pb dating results from the Velay granites and the Lower Gneiss Unit (LGU). See legend of Figure 4 for explanations.

Fig. 6. LA-ICPMS zircon U-Pb dating results from the granite dikes crosscutting the base of the UGU. See legend of Figure 4 for explanations.

Fig. 7. Comparative zircon Th/U ratio of the concordant analyses vs their $^{206}Pb/^{238}U$ date. The background curves correspond to kernel density plots of concordant $^{206}Pb/^{238}U$ dates. (A) UGU. (B) LGU and Velay granites. (C) Granite dikes.

Fig. 8. Comparative εHf diagrams showing the results of combined U-Pb and MC-LA-ICPMS Lu-Hf isotopic analyses on zircons from the Tournon area: (A) UGU, (B) LGU and Velay granites, (C) Granite dikes. All uncertainties are given at 95% confidence (2σ). The colored Kernel Density Estimates represent the distribution of $^{206}Pb/^{238}U$ dates for spots that were also analyzed for Lu-Hf isotopes; while the dashed ones correspond to the whole dataset.

Fig. 9. Compilation of all Zircon U-Pb LA-ICPMS dating results from the Tournon area. (A) Tera-Wasserburg diagrams. The darkest areas correspond to the highest densities of ellipses. Ellipses in red highlight the Archean to Paleoproterozoic zircons. The background grey shaded area depict the field of discordant Archean to Paleoproterozoic zircons and its extension to a Neoproterozoic lower intercept. (B) Kernel density plot (black line) and probability density plot (orange line) of concordant $^{206}Pb/^{238}U$ dates (for dates < 1.2 Ga) or $^{207}Pb/^{206}Pb$ dates (for dates > 1.2 Ga) showing the main zircon forming events recorded in the Tournon area. The corresponding well-recognized Earth-scale geodynamic events are indicated for reference.

Fig. 10. Compilation of combined U-Pb and Lu-Hf isotopic data in zircons of all samples from the Tournon area (blue symbols, sorted according to tectono-stratigraphic units and rock type). Fields of data for the Arabian-Nubian Shield (ANS) is from Morag et al. (2011b), the Cadomian arc is from Samson et al. (2003), and the West African craton are from Block et al. (2016) (Léo-Man rise; box 1) and Eglinger et al. (2016) (Kénéma-Man domain; boxes 2 and 3) and unpublished data from O. Laurent (Amsaga terrane; box 3). Data from the Cambrian sediment from Morocco are from Avigad et al. (2012) and Cambrian sediments from Israel are from Morag et al. (2011a). Data from Cadomian sediments in Germany are from Linnemann et al. (2014). The yellow arrows represent the isotopic evolution of continental crust (calculated using an average "crustal" $^{176}Lu/^{177}Hf$ ratio of 0.0115) formed during the two main events of crust formation in the Gondwana supercontinent, i.e. 3.4-3.1 Ga and 2.3-2.0 Ga (e.g., Kemp et al., 2006). DM field is bounded by the models of Griffin et al. (2002) for the upper limit and Naeraa et al. (2012) for the lower limit. The probability density plot along the x-axis shows the distribution of U-Pb dates of the zircons from the Tournon area and highlight the successive orogenic episodes recorded thereby (LAO – late-Archean orogens; EO – Eburnean Orogen; PO – Pan-African orogens; VO – Variscan Orogen).

Fig. 11. Diagram of zircon $^{176}Hf/^{177}Hf_t$ vs. $^{206}Pb/^{238}U$ date for samples *TN12* (banded gneiss) and *TN13* (amphibolite) of the UGU, with emphasis on the relationship between the ca. 480 Ma zircons and the ca. 345 Ma zircons. Plain arrows indicate the expected evolution of the $^{176}Hf/^{177}Hf$ ratio of the bulk samples, considering $^{176}Lu/^{177}Hf$ ratios typical of mafic material (= 0.025) for the amphibolite and of average crustal material (= 0.015) for the banded gneiss. The black dashed arrow represents the evolution of the $^{176}Hf/^{177}Hf$ ratio in zircons of sample *TN13*, using the average $^{176}Lu/^{177}Hf$ ratio measured in zircons from this sample (= 0.002). Many 380-340 Ma-old zircon rims and grains from *TN13* show significantly lower $^{176}Hf/^{177}Hf$

ratios than what is predicted from zircons recrystallization (black dashed arrow), indicating that their formation requires the input of externally-derived, non-radiogenic Hf, most likely derived from the surrounding gneisses (represented by *TN12*).

Fig. 12. Comparison of detrital zircon U–Pb dates from Cambrian–Ordovician sandstones of northern Gondwana mainland and from gneisses of the Tournon area. (A) kernel density plot of concordant $^{206}Pb/^{238}U$ dates (for dates < 1.2 Ga) or $^{207}Pb/^{206}Pb$ dates (for dates > 1.2 Ga). (B) non-metric multi-dimensional scaling plot of the north Gondwana and EMC dataset (Vermeesch, 2013). Data have been compiled by Meinhold et al. (2013) and are from: Avigad et al. (2012; Morocco), Linnemann et al. (2011; Algeria), Meinhold et al. (2011; Libya, Murzuq Basin), Meinhold et al. (2013; Libya, Kufra Basin), Kolodner et al. (2006; Israel and Jordan).

Fig. 13. (A) Schematic diagram summarizing the U-Pb zircon results obtained in the Tournon area. Bold ages correspond to the age of granite or gabbro emplacement, or of migmatization. Age ranges in italic are only constrained by few scattered data points. Data from the granite dikes have been underlined only to facilitate reading of the figure. [1]ages from Laurent et al. (2017). (B) Synopsis of sedimentary, metamorphic and magmatic events recorded by zircons from the Tournon area.

Appendices

ESM 1. Sample descriptions, field photographs and sample location coordinates.

ESM 2. Analytical methods for U-Pb and Lu-Hf analyses.

ESM 3. Detailed description of the U-Pb and Lu-Hf data.

ESM 4. Table of U-Pb data.

ESM 5. Table of Lu-Hf data.

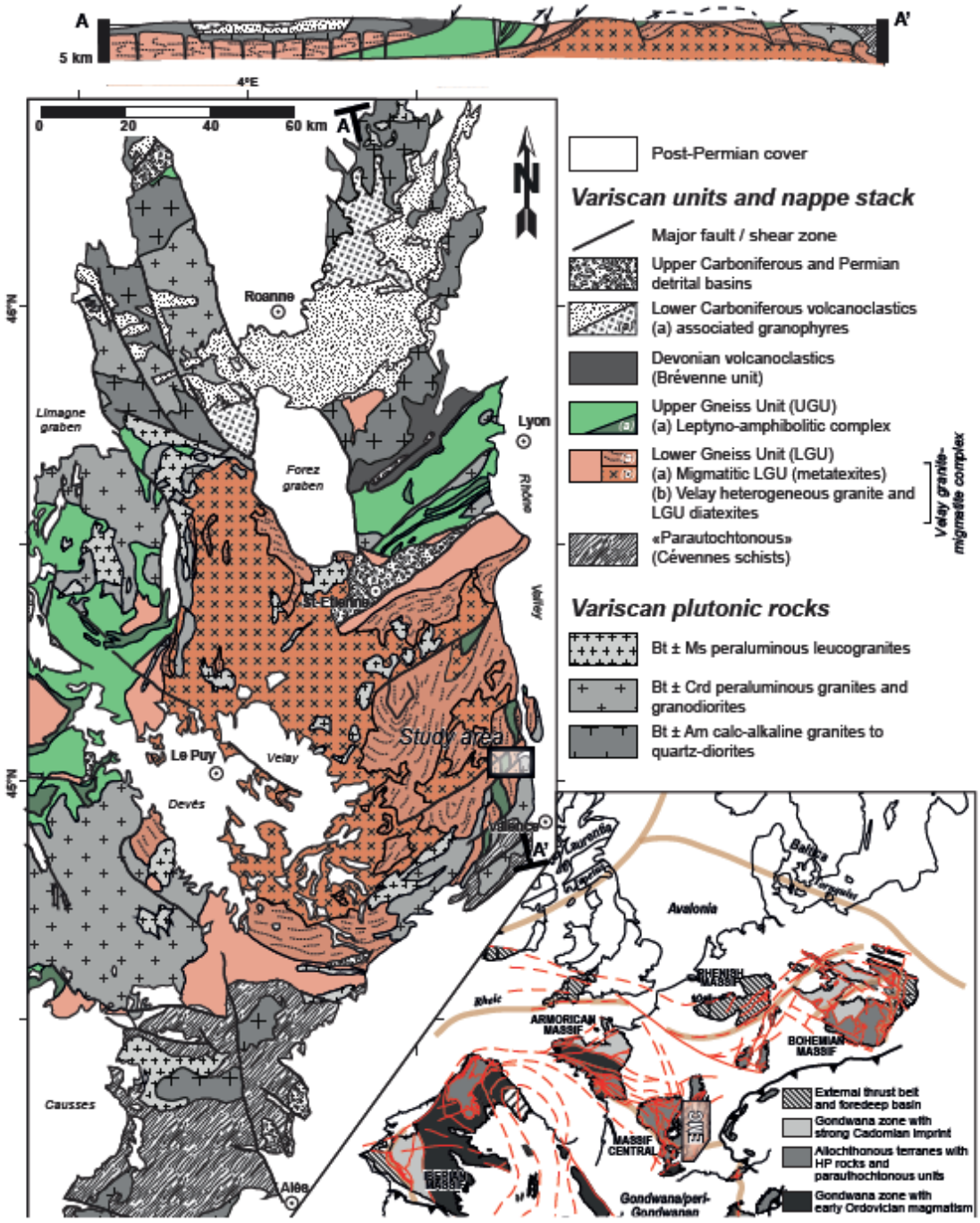

Fig. 1

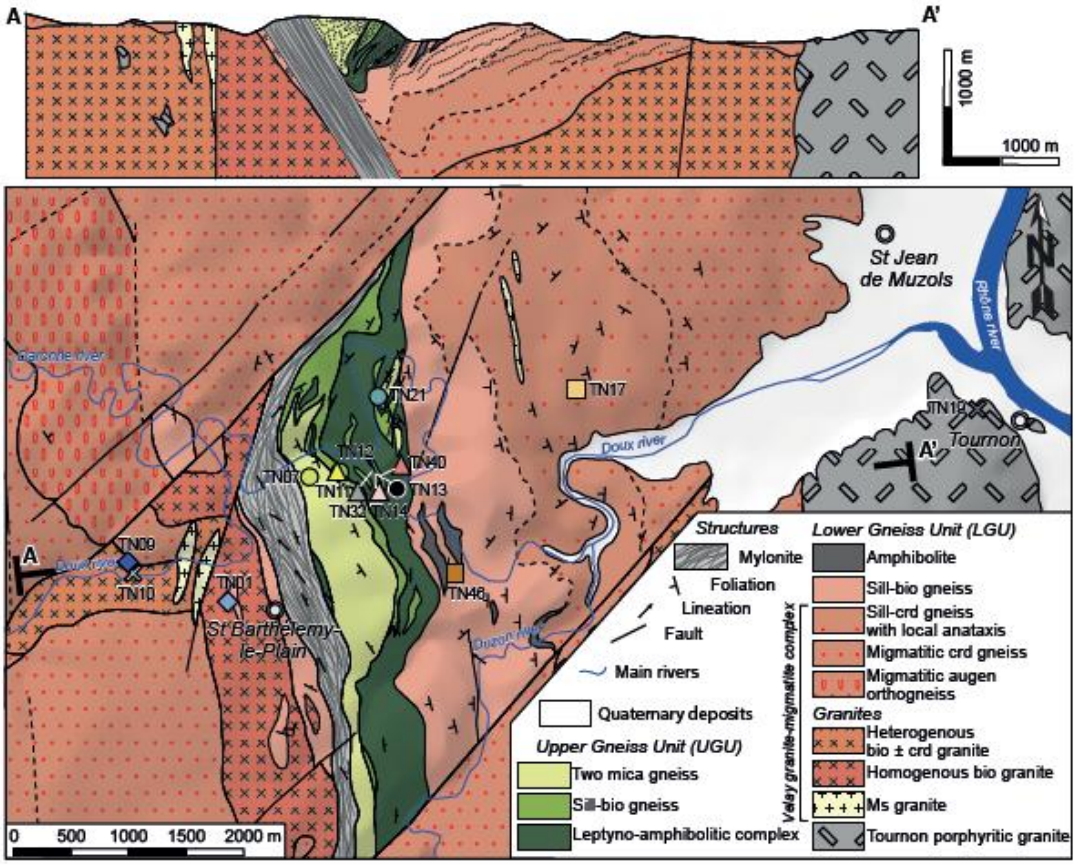

Fig. 2

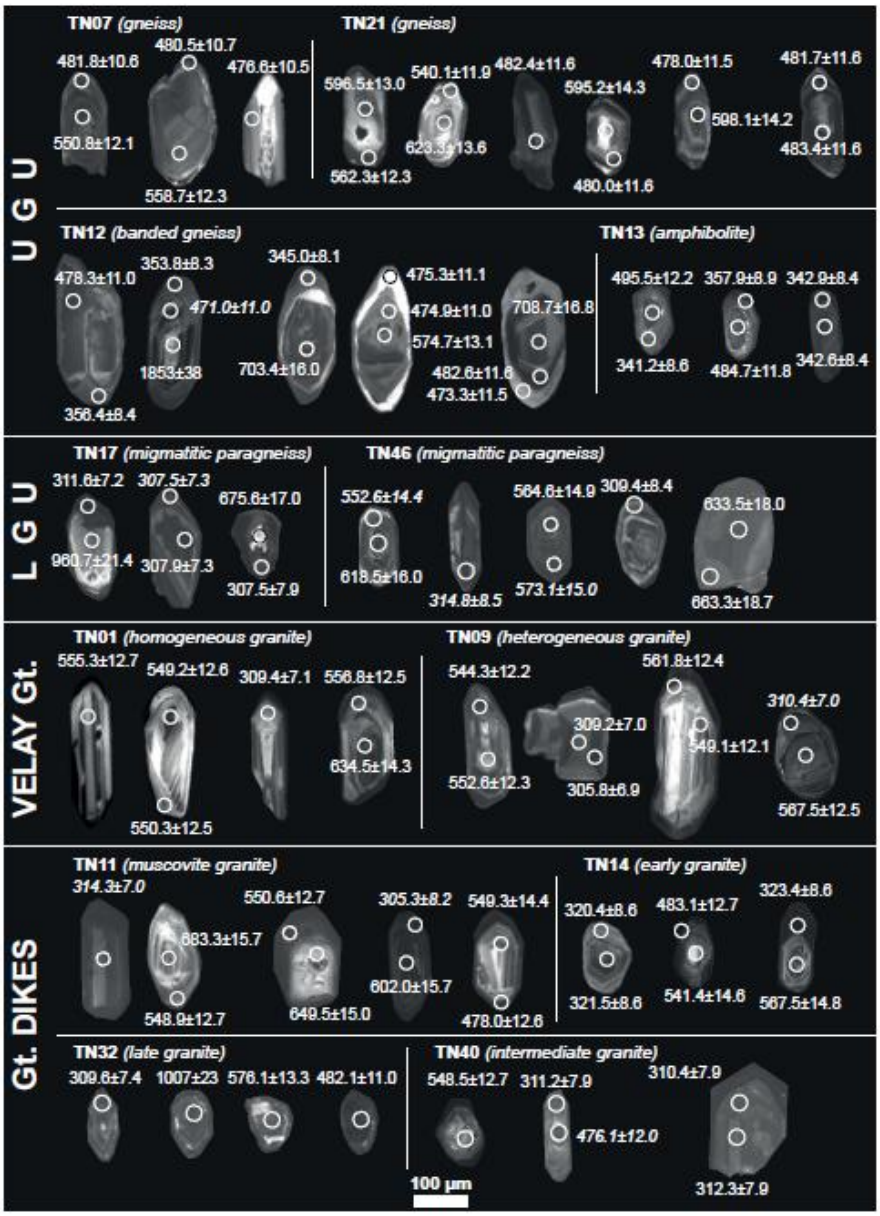

Fig. 3

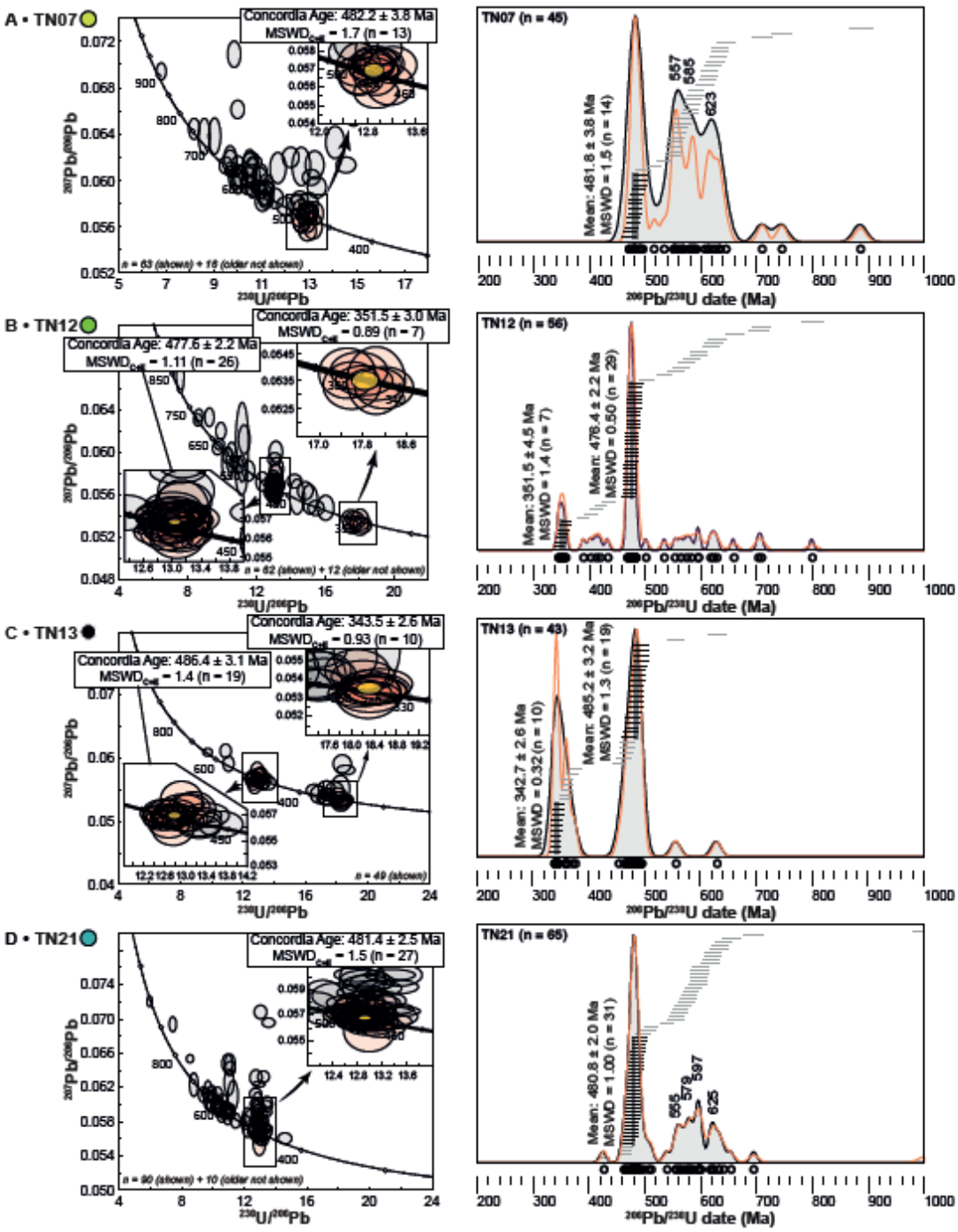

Fig. 4

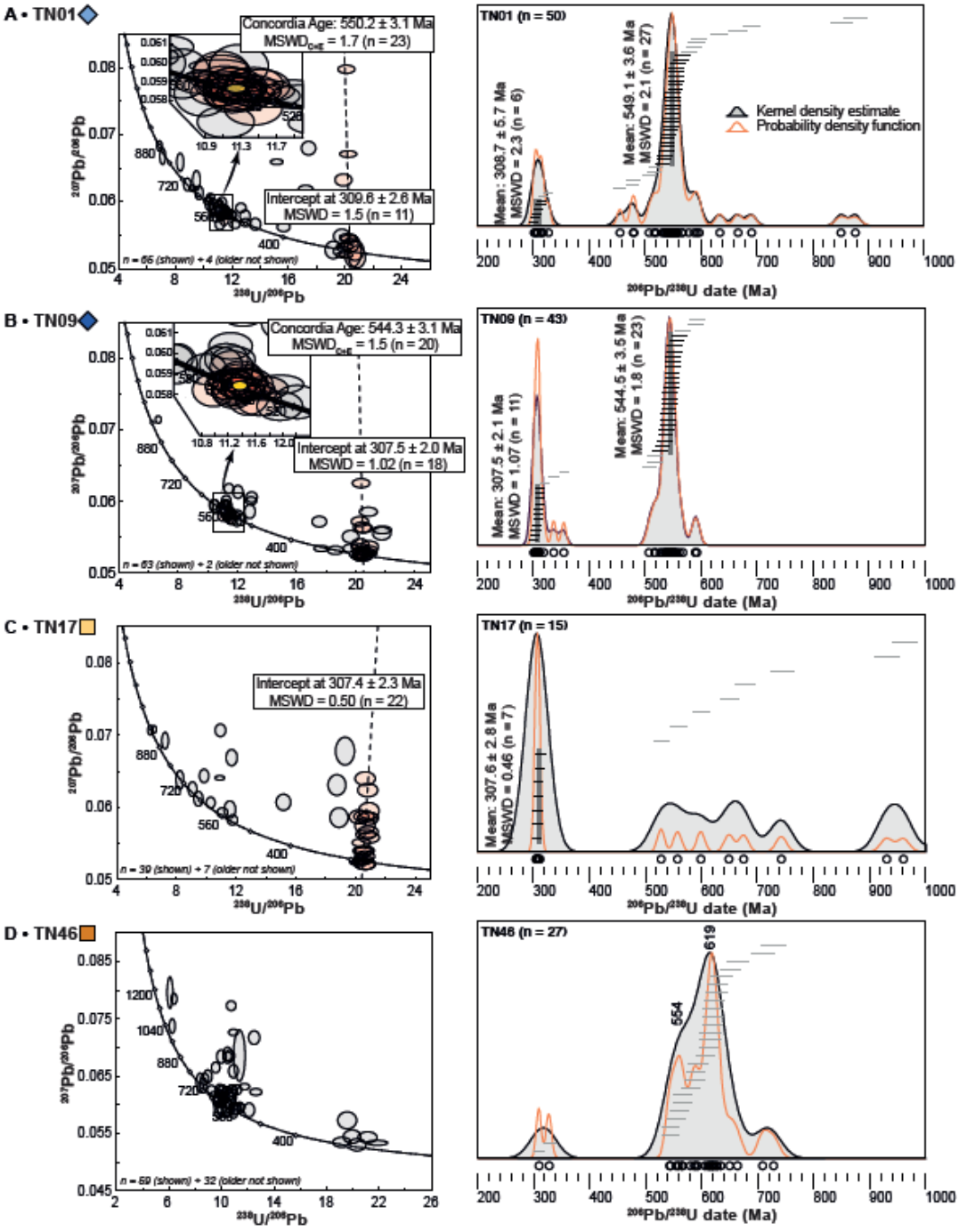

Fig. 5

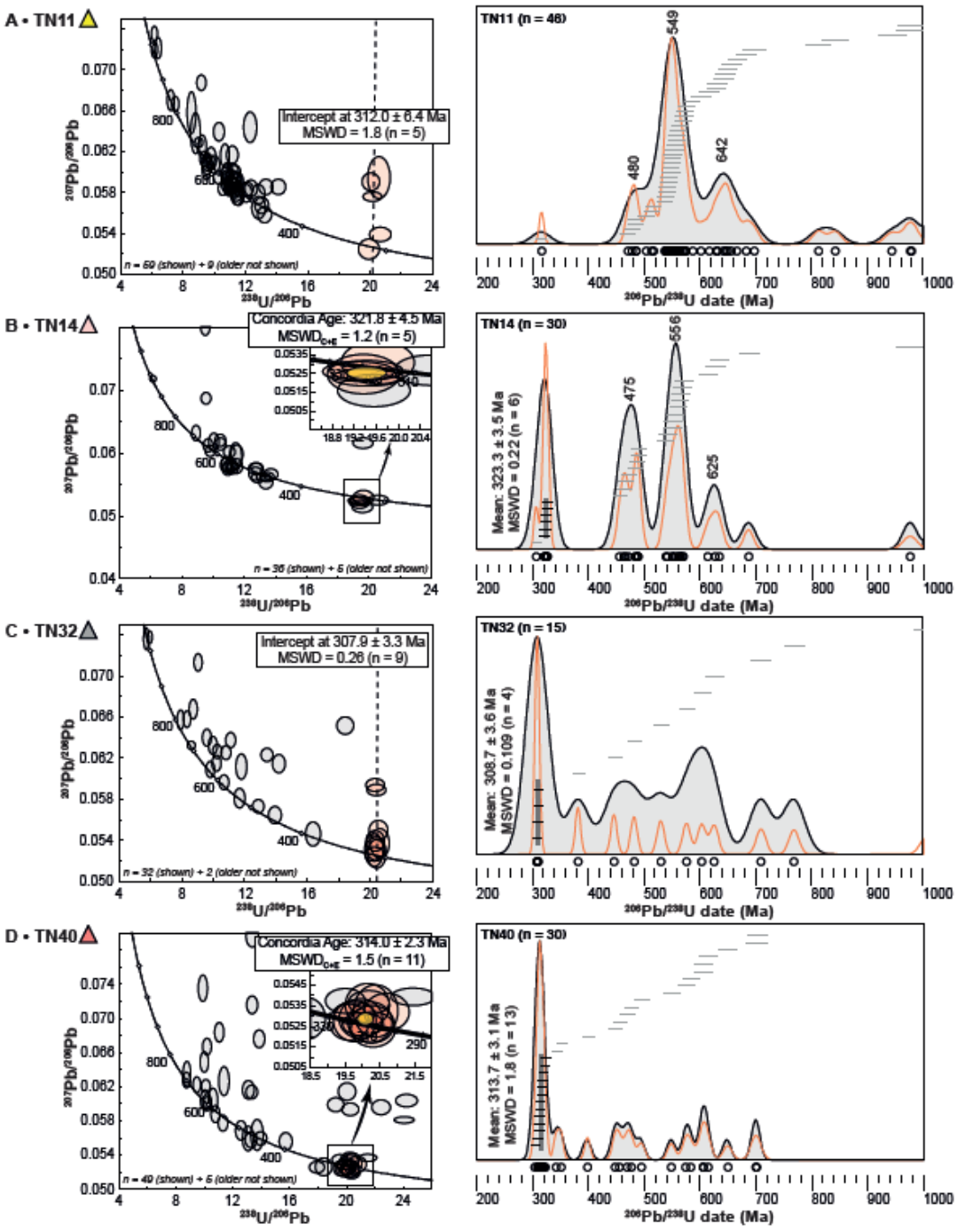

Fig. 6

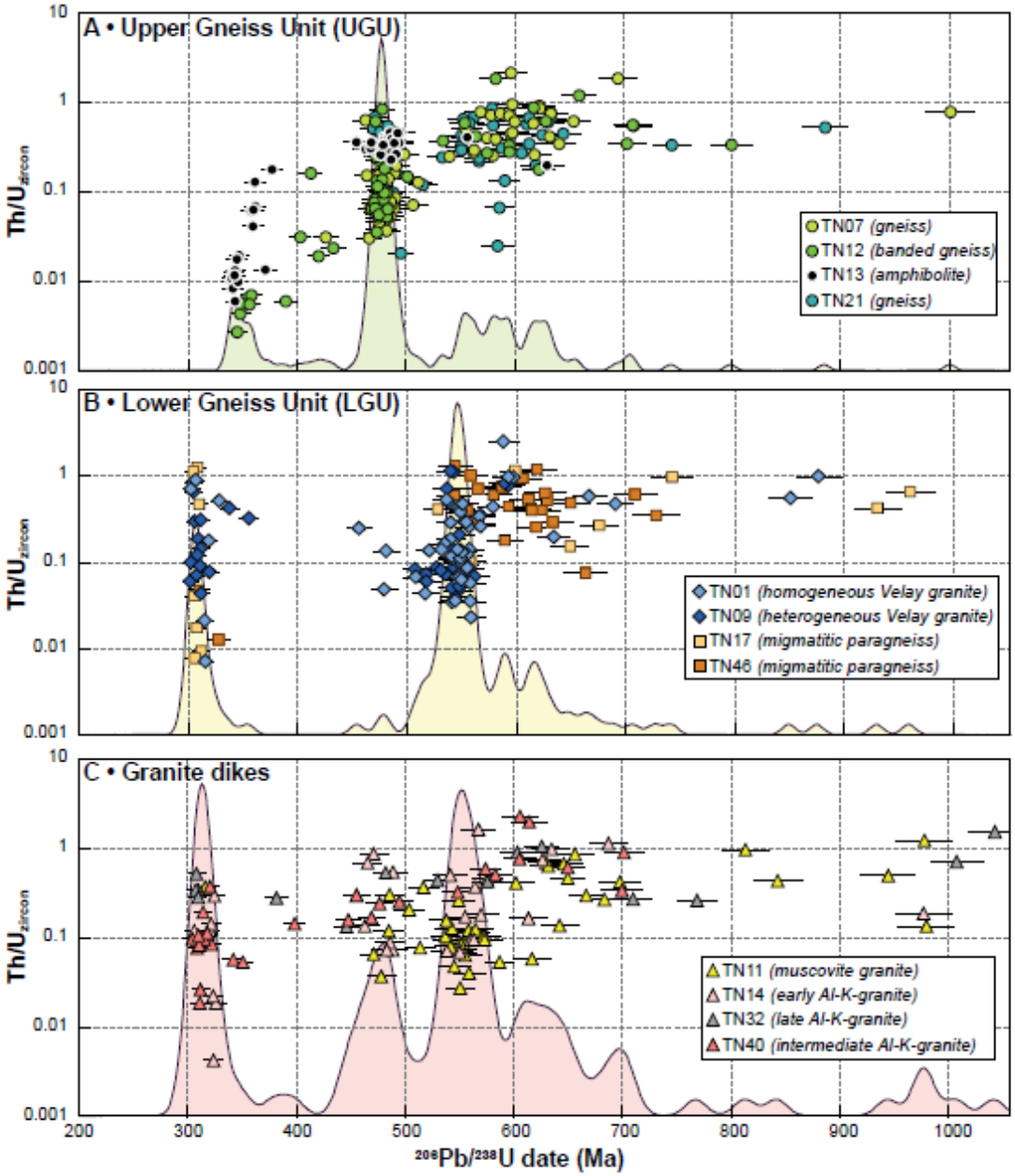

Fig. 7

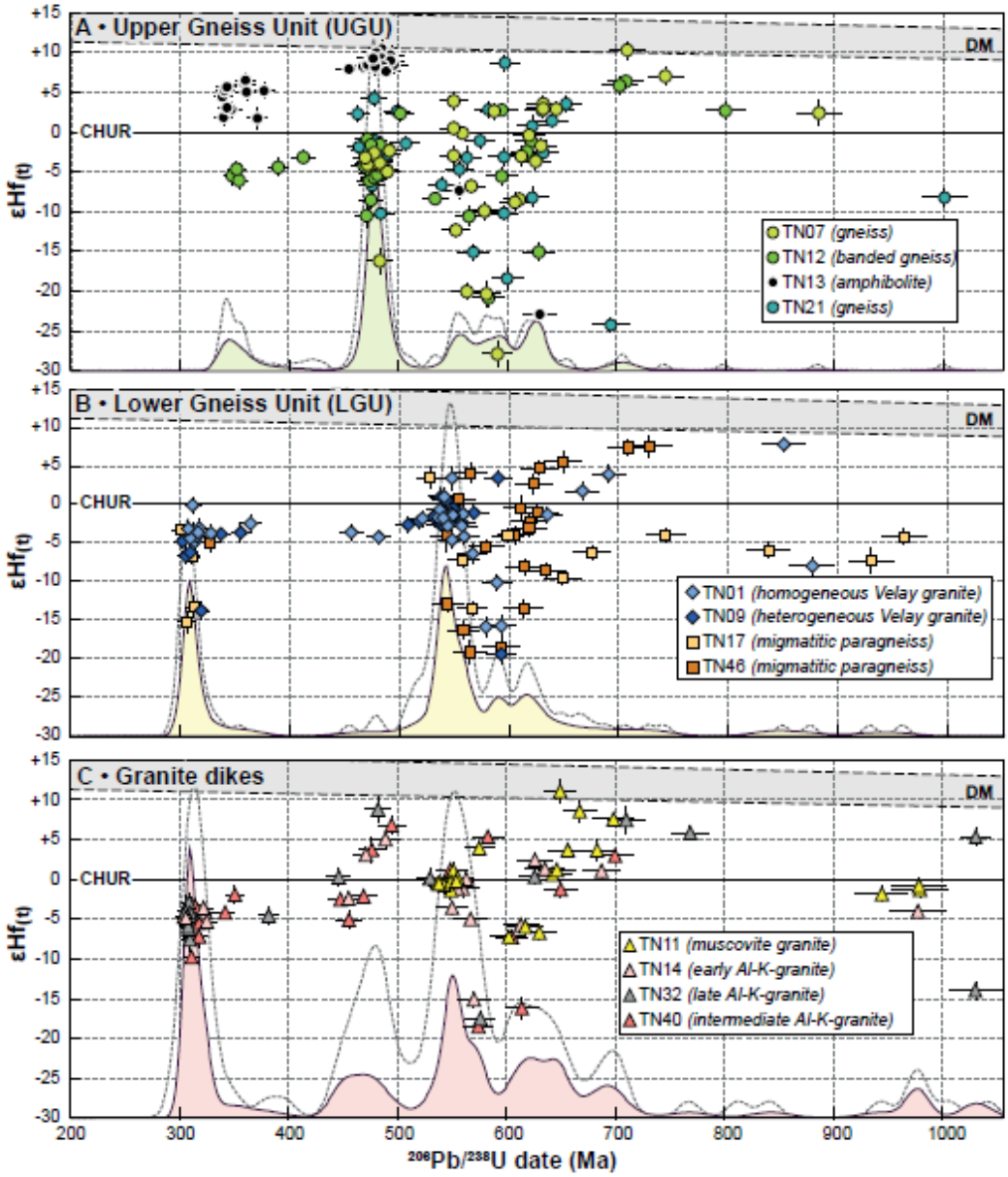

Fig. 8

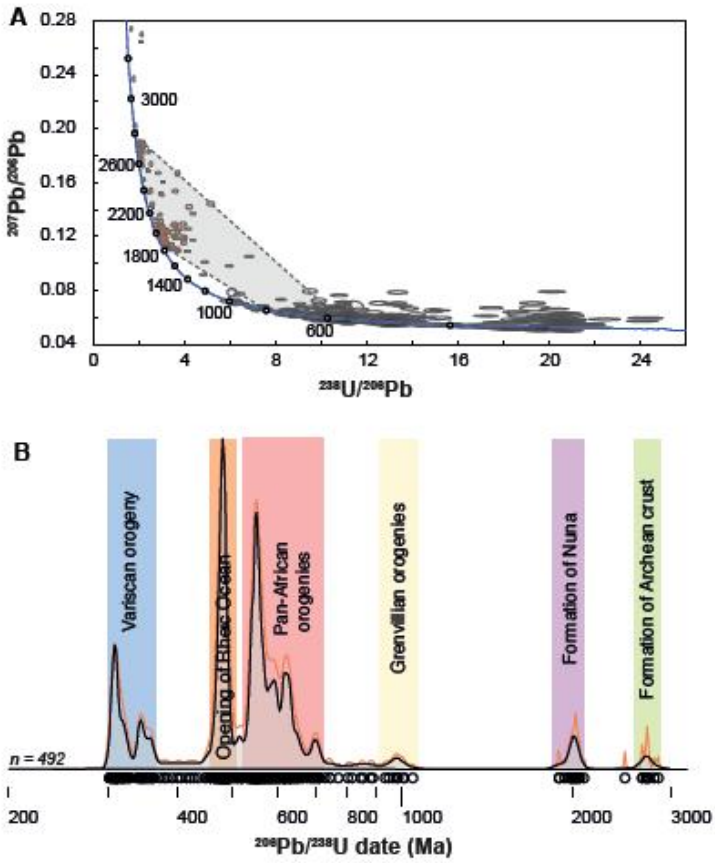

Fig. 9

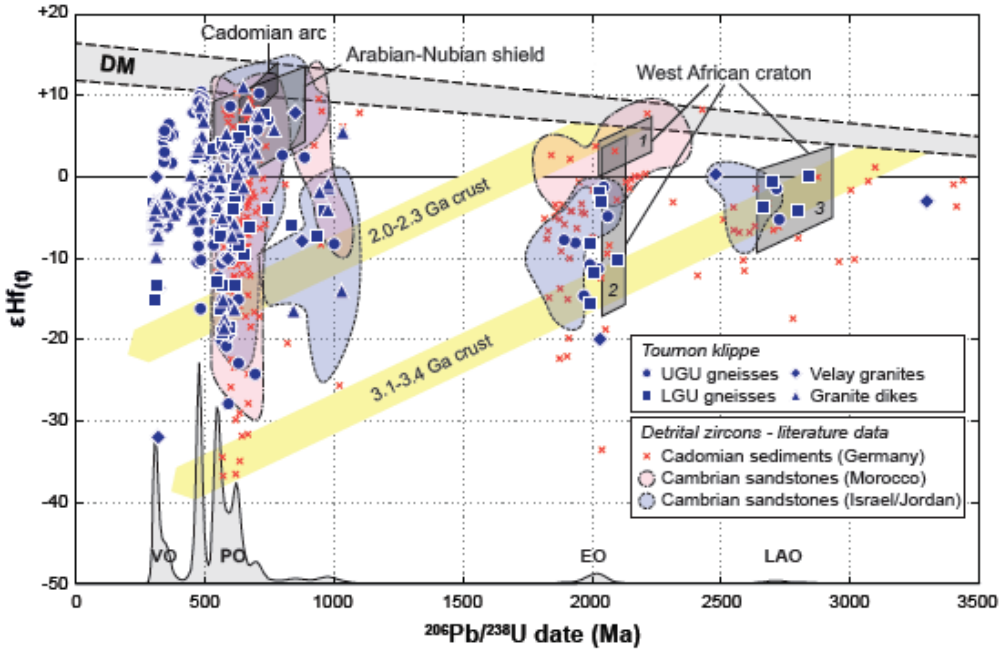

Fig. 10

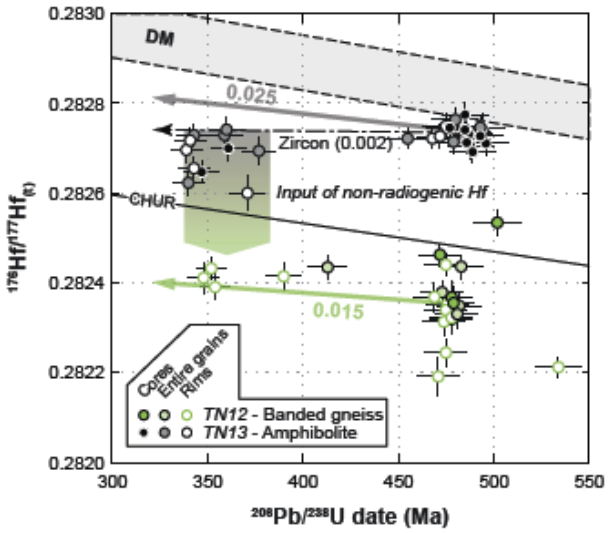

Fig. 11

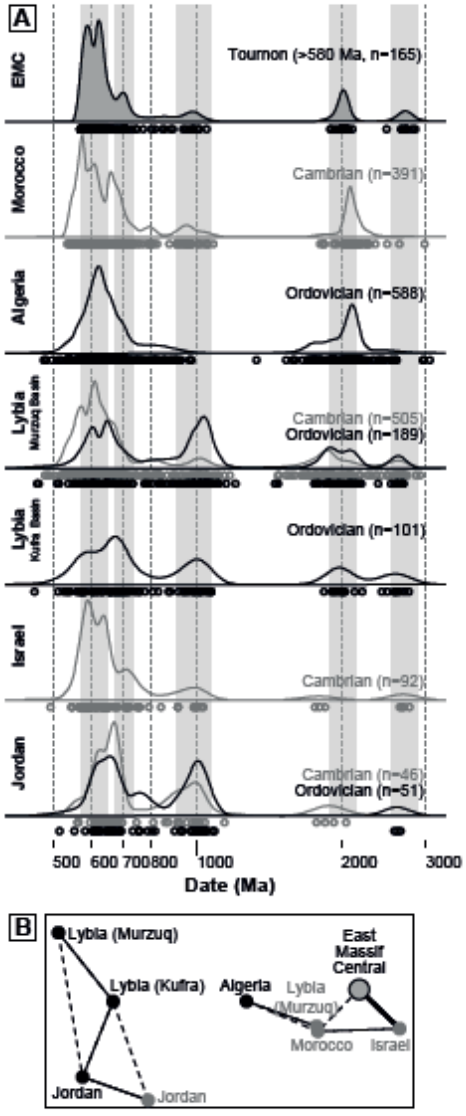

Fig. 12

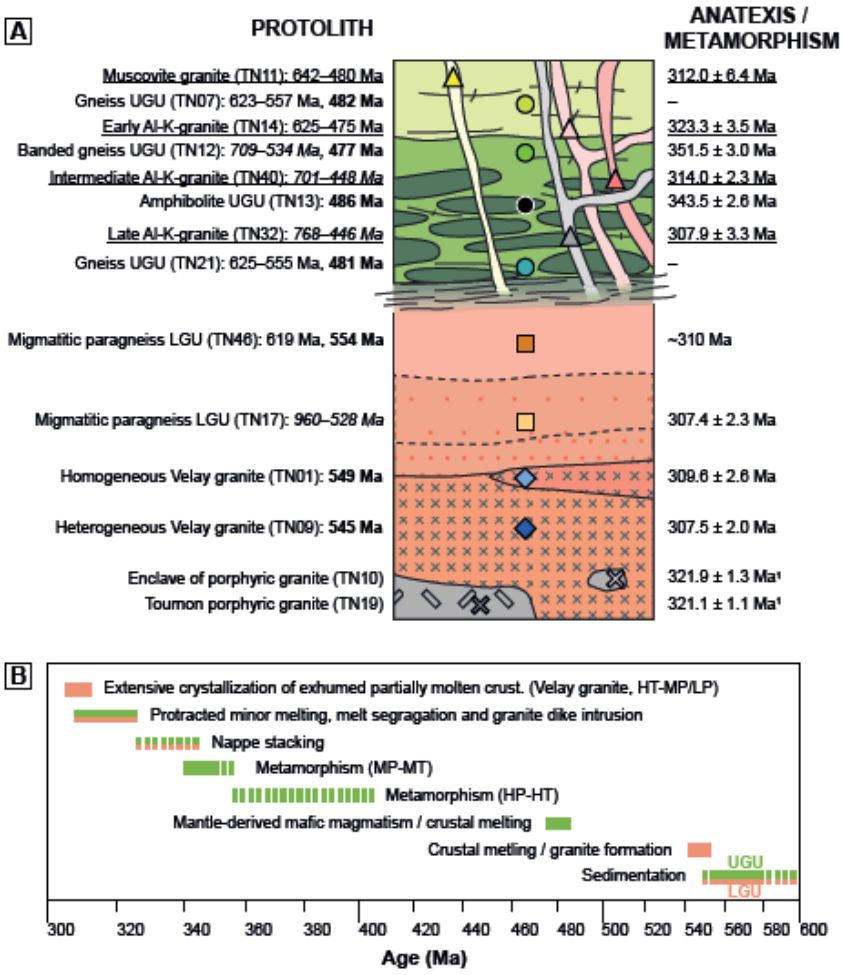

Fig. 13

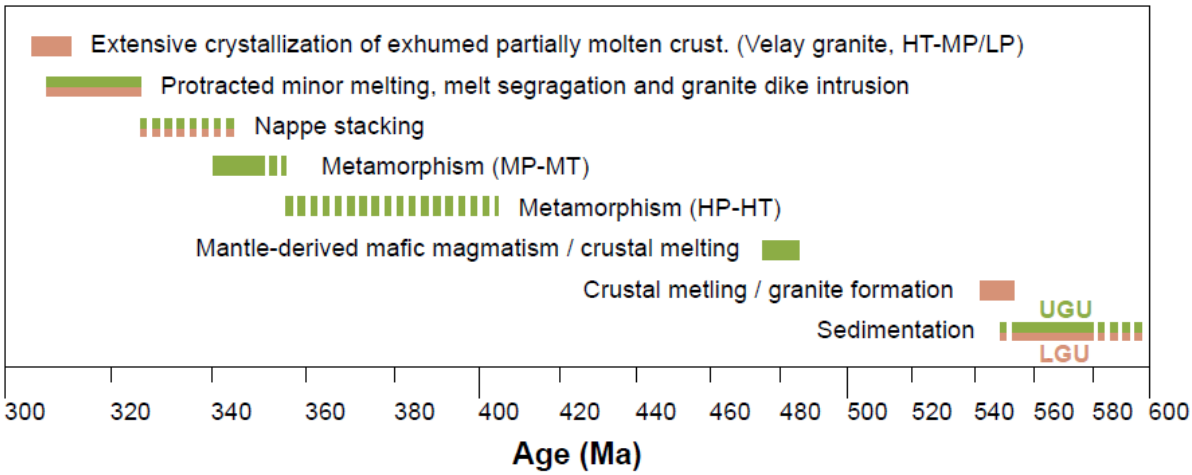

Graphical abstract

Highlights

- We present new U-Pb zircon ages Lu-Hf isotopes from the East Massif Central (EMC)
- We present a timeframe for sedimentary, magmatic and metamorphic events
- The EMC crust derives from a Cadomian Gondwana-sourced sedimentary basin